NASA TECHNICAL MEMORANDUM   NASA TM-77855

CONTRIBUTION TO THE STUDY OF THE ELECTRIC ARC
EROSION OF METALLIC ELECTRODES

A. Castro

NATIONAL AERONAUTICS AND SPACE ADMINISTRATION
WASHINGTON, D.C. 20546   MAY 1985

1. Report No. NASA TM-77855	2. Government Accession No.	3. Recipient's Catalog No.
4. Title and Subtitle CONTRIBUTION TO THE STUDY OF THE ELECTRIC ARC - EROSION OF METALLIC ELECTRODES		5. Report Date May 1985
		6. Performing Organization Code
7. Author(s) A. Castro		8. Performing Organization Report No.
		10. Work Unit No.
9. Performing Organization Name and Address Leo Kanner Associates Redwood City, CA 94063		11. Contract or Grant No. NASw-4005
		13. Type of Report and Period Covered Translation
12. Sponsoring Agency Name and Address National Aeronautics and Space Administration, Washington, D.C. 20546		
		14. Sponsoring Agency Code

15. Supplementary Notes

Translation of "Contribution à l'étude de l'arc électrique - Erosion des électrodes métalliques," Paris XI. Université de Paris-Sud. Orsay, France, Thesis, January 12, 1978, pp. 1-82

(A79-23426)

16. Abstract

Electrode erosion is a complex phenomenon found in industrial devices (contactors, breakers) and in scientific devices (spectroscopic arcs). In industrial devices, part of the erosion is due to the transfer of matter. This is due to the metallic bridge formed and broken when the contacts open. Another part of the erosion is due to the electric arc and this aspect is the subject of this thesis. Electrode erosion is generally measured by weighing, but this method is long, often inconvenient. It is still used as a reference, however. We developed a spectrosocpic method for performing this measurement. It consists of measuring the intensity of a spectral emission line of the arc itself, and therefore with minimum practical constraints. This method is based on three assumptions: 1) the optical transparency of plasma; 2) knowledge of the law of temperature variations as a function of the arc current; 3) the relationship between the intensity of a spectral emission line of the electrode material and the erosion rate.

17. Key Words (Selected by Author(s))	18. Distribution Statement Unclassified-Unlimited	
19. Security Classif. (of this report) Unclassified	20. Security Classif. (of this page) Unclassified	21. No. of Pages 63	22.

ACKNOWLEDGEMENTS

TABLE OF CONTENTS

CONTRIBUTION TO THE STUDY OF THE ELECTRIC ARC - EROSION OF METALLIC ELECTRODES

A. Castro

CHAPTER 1 - INTRODUCTION

Electrode erosion is a complex phenomenon found in industrial devices (contactors, breakers) and in scientific devices (spectroscopic arcs).

In industrial devices, part of the erosion is due to the transfer of matter. This is due to the metallic bridge formed and broken when the contacts open.

Another part of the erosion is due to the electric arc and this is the topic of this thesis.

Electrode erosion is generally measured by weighing, but this method is long, often inconvenient. It is still used as a reference, however.

We developed a spectroscopic method for performing this measurement. It consists of measuring the intensity of a spectral emission line of the arc itself, and therefore with minimum practical constraints.

The method is based on three assumptions which are:

-the optical transparency of plasma. To check this, we developed an original device.

-knowledge of the law of temperature variations as a function of the arc current. This is studied based on the relative intensity ratio.

---

*Numbers in the margin indicate pagination in the original text.

-the relation between the intensity of a spectral emission line of the electrode material and the erosion rate. To check this assumption, we used three materials: sliver, copper and nickel. This choice is guided by the concern to find a meterial which may replace silver in the construction of contacts and/or reduce erosion.

Our prime concern is to find out whether there is a relation between the intensity of an emission line of the electrode material and the erosion rate, based on the assumptions pertaining to the optical transparency and temperatures. Then, we compare the different materials from the standpoint of erosion.

CHAPTER 2 - REVIEW OF ELECTRIC ARCS   /3

2.1 INTRODUCTION

An arc is a discharge into a gas. However to place an arc in terms of other discharges, it is interesting to plot the curve V = f (I), where V is the voltage at the electrode terminals free of points or very sharp edges and I is the discharge current (figure 1).

Figure 1 - Diagram of a gaseous discharge

There are three main ranges with transitions where the discharge is somewhat unstable. These three ranges are called: I, the Townsend discharge; I, the luminescent discharge; II, the arc discharge. Depending on the pressure, the arc discharges are called low pressure or high pressure arcs. One of the features of high pressure arcs is that the electron, ion and the substance temperatures have approximately the same value, as shown in figure 2 according to (1).

Figure 2 - Gas temperature (Tg) and electron temperature (Te) in the positive column of a mercury steam arc as a function of the pressure.

The situation is different at low pressures where the electron temperature is two orders of magnitude higher than the ion and gas substance temperature. This is because the electrons, which have a long average free path, receive high energy from the electric field and lose little in the collisions because of their small size and mass. Therefore, we now only distinguish high pressure arcs.

We distinguish three regions in an arc of this type: the   /5

3

cathode region, the anode region and the positive column (figure 2).

Figure 3 - Distirbution of field E
and potential V between
cathode and anode.

If we plot the potential in the arc as a function of the dis-
tance to the cathode, we find a distribution such as that in figure
3b where there is a voltage drop near the cathode, a voltage drop
in the volumn and near the anode.

From the potential curve, we may plot the electric field distri-
bution in the arc, figure 3c. The curve is exaggerated, because in
reality the electric field near the electrodes has values which are
several orders of magnitude larger than in the column.

2.2 - THE POSITIVE COLUMN

In regard to the positive column, several theories were built
on the model of a cylindrical and uniform column, for the low pres-
sure or high pressure arc, where:

4

a) the electrodes are very far from the part under consideration,

b) the neutral gas around the column is immobile, homogenous and convectionless.

In the study of high pressure and stationary arcs based on assumptions 1, 2, there are two types of arc models: radiative and nonradiative arcs.

Nonradiative Arc

In the high pressure and stationary radiative arc model, the equation for the energy balance, called Elenbass-Heller's equation, is expressed:

$$\sigma E = -\frac{1}{r}\frac{d}{dr}\left(rK\frac{dT}{dr}\right) \qquad 0 \leq r \leq R$$

where σ is the electric conductivity, K is the thermal conductivity, E is the axial electric field which is considered uniform, T the temperature which is a function of the distance r to the axis only, R the column radius.

The left term is the heat due to the Joule effect, whereas the right term is the heat transfer due to thermal conduction.

The resolution of this equation is fairly difficult because σ and K depend on the temperature. To solve it, one must do approximations which are also models, namely:

-the parabolic model where σ and K are independent of the temperature, which makes the solution easy:

$$T = T_P + \frac{E^2 R^2}{4K} \quad \text{with } T_P = \text{wall temperature at } r = R$$

-the logarithmic model where σ is assumed to be dependent upon

temperature only at the center of the column and nil elsewhere, which leads to a solution of the following type:

$$T - T_p = - \frac{A}{K} \ln \left(\frac{r}{R}\right) \qquad \text{with } \sigma(r)=0 \quad \text{for } r \neq 0$$

where A is a constant and it is assumed that K is independent of T, T_p being the wall temperature at $r = R$.

   -the canal model where one assumes there is a symmetrical and uniform ionized canal about the axis, with the parabolic model valid inside the canal and the logarithmic model valid outside of it.

Radiative Arcs

   In the high pressure and stationary radiative arc model, the radiated power may be disregarded. This leads us to express Elenbass-Heller's equation, modified by a term which accounts for radiation, namely:

$$\sigma E^2 - P_r = - \frac{1}{r} \frac{d}{dr}\left(rK\frac{dT}{dr}\right)$$

P_r is the radiated power density. The inclusion of this term complicates the solution of Elenbass-Heller's equation even more, because this adds problems such as the existence of the thermodyanmic balance.

Real Arcs

   In real cases, one finds several complications such as that due to the presence of gas surrounding the arcwhich is not immobile, but is moving (convection) with respect to the electrode walls. The natural convection in high pressure arcs is incompatible with the cylindrical revolution symmetry when the arc is horizontal and with the equality of the sections when it is vertical.

6

A numerical approach was performed by LOWKE (2), for the case of a vertical arc in air, to calculate the temperature and the axial and radial velocities of plasma.

2.3 REGIONS CLOSE TO THE ELECTRODES

We shall now review the features and problems occurring in regions close to electrodes exhibiting a metal-gas transition, as well as phenmonena called plasma jets.

2.3.1 - Cathode Region: the features are:

a) A high current density (10^2-10^7 A/cm^2) which was estimated either by measuring the path left by the electrode on the surface, or by measuring the luminous surface of the arc base.

b) A potential drop on the order of 10-16V and measured by mobile probes or by oscillographic recordings of the arc voltage when the electrodes opened or closed (reference (3), (4).

The main theoretical problem is to know the mechanism of producing charges which are compatible with the high current densities observed. One of the main mechanisms assumed, given the value of the cathode drop and the dimension (similar to the mean electronic free path), is the field effect emission. The current density is thus given by NORDHEIM-FOWLER's equation as a function of the electric field (5) for a temperature T = 0

$$j_e = j = 1.54 \times 10^{-6} \frac{E_c^2}{\Phi} \exp \left(- 6.8 \times 10^7 \frac{\Phi^{3/2}}{E_c}\right) (1) \quad (A/cm^2)$$

where J_e is the current density, E_c the electric field at the cath-
ode, Φ the discharge energy of the cathode material. It is interesting to compare (see figure 4) the current density due to the field effect emission with that due to the space charge of positive ions calculateed by MACKEOWN (6) from Poisson's equation applied to the cathode sheath, namely:

$$E_c^2 = 7.6 \times 10^5 \, V_c^{\frac{1}{2}} \, [j_+ \times (\frac{m_+}{m_e})^{\frac{1}{2}} - j_e] \qquad (2)$$

where m_+ is the ion mass, m_e the electron mass, V_c the cathode drop, j_+ the ion current density

ELECTRONIC CURRENT DENSITY A/cm2

Figure 4 - Electric field at cathode as a function of
the electronic current density given by
NORDHEIM-FOWLER (F-N) and MACKEOWN's equation,
according to reference (40).

In figure (4), the equation (1) is represented for three dis-   /11
charge energy values. Equation (2) is represented for a $\frac{J_+}{j_e}$ value
of 0.01

8

We see that the electric field produced by positive ions is insufficient for sustaining a field effect emission even if the discharge energy is 2 eV.

The increase of the electric field, due to the effect of sharp edges or points which could promote the emission, was examined by ECKER (5). However, it seems that they have little influence on the total emission. Furthermore, the thermoionic emission mechanism was described, based on the upper boiling temperature of the cathode. The electronic current density is therefore given by RICHARDSON's law:

$$j_e = AT_c^2 \exp \left\{ - \frac{e\Phi}{kT_c} \right\} \tag{3}$$

A being a constant, T_c the cathode temperature.

Since certain materials show current densities incompatible with this law, the arcs were classified:

1) thermoionic emission arcs where the cathode temperature is high enough to sustain a thermoelectronic emeission with little evaporation from the electrode.

2) cold cathode arcs, where the cathode temperature does not /12 permit an adequate thermoionic emission, but which evaporates intensely. The emission mechanism is probably due to the field effect.

A more refined theory for explaining the cold cathode arcs was proposed by LEE (7) in 1959 using MURPHY and GOOD's work (8), which explained that the total current density is:

$$j = e \int_{W_0}^{\infty} D(E,W)N(W)dW \tag{4}$$

where D (E,W) is the probability of emission of an energy electron W, N(W). The number of electrons per second has a energy W, to the nearest W_o, the potential energy of electrons in metal. A more explicit expression is given by ROHRBACK (9):

$$j(T,E,\Phi) = \frac{4\pi mkT}{h^3}\left[\int_{W_0}^{W_1}\frac{\ln\{1+\exp[-(W+\Phi)/kT]\}}{1+\exp\{8\pi/\overline{2m}\,v(y)W^{-2}/3heE\}}\,dW + \int_{-W_1}^{\infty}\ln[1+\exp(-(W+\Phi)/kT)]\,dW\right]$$

$$W_1 = \frac{W_{max}}{\sqrt{2}}$$

electron mass and charge

BOLTZMAN's constant

PLANK's constant

$$W_{max} = \sqrt{\frac{Ee^3}{4\pi\varepsilon}}$$

Electric field

$$y = \frac{W_{max}}{|W|}$$

This theory gives a satisfactory explanation in certain cases, /13 such as Cu. However, there are cases such as that of mercury, which cannot be explained by this theory.

This theory is general and shows (Ref. 8) that expression (4) leads to:

1) expression (1) already mentioned for T = 0

2) the field emission formula with temperature correction when we have the condition $T < 0.75 \times 10^{-6}E$, E being the electric field in volts per meter.

$$j(E,T,\Phi) = \frac{AE^2}{\Phi\,t(y)}\frac{\pi CT}{\sin\pi CT}\exp\left\{-\frac{4\sqrt{2}\,\Phi^{\frac{3}{2}}v(y)}{3E}\right\}$$

$$C = \frac{2\sqrt{2\Phi}\,t(y)}{E}$$

10

3) the thermoionic emission expression (Richardson-Schottky's law) when we have the condition $T \geqslant 0.75 \times 10^{-6} E$.

$$j(E,T,\Phi) = AT^2 \frac{\pi d}{\sin \pi d} \exp\left[-\frac{\Phi - B\sqrt{\overline{E}}}{kT}\right]$$

$$d = \frac{E^{\frac{3}{4}}}{\pi T}$$

A theory of the field effect emission applied to arcs, called /14 individual field emission, was established by ECKER (1), by considering the field on a point of the electrode surface which varies in time because of statistical variations of the space charge.

The electronic emission process due to Auger's effect was reported by HAGSTRUM (11) and may be summarized as follows: when an ion approaches the cathode, it modifies the potential barrier and a metal electron may exit and neutralize the ion and at the same time release energy which goes to another electron in the metal conduction band. It is evident that the second electron is placed only if $E_i \geq 2\Phi$, Since E_i is the ionization energy of the incident ion and Φ the metal's discharge energy, its kinetic energy will be between $E_i - 2\Phi$ and $E_i - 2\varepsilon o$, εo being the lowest energy level in the metal conduction band, starting from a no-load level.

Photoelectric emission is possible, but the yield is low: on the order of 10^{-1} electron/quantum in the case of Ni and Cu in U.V. (700Å), value given by WEISSLER (12). The average energy required in this case, to release an electron by photons, is on the order of 10^2 eV/electrons. These two mechanisms have low yields and do not contribute very much to the emission of a cold cathode.

Another possibility of releasing elecrons from the cathode

11

bombarding it with excited atoms. The excitation energy of these atoms must be greater than the metal's discharge energy. Von ENGEL and ROBSON (13) built a theory of arcs to explain the emission of a cold cathode, using this possibility, but according to ECKER's analysis (10), this theory depends on the coexistence of several favorable factors, namely:

-a high atom density opposite the cathode,
-the radiation of these atoms should go toward the cathode,
-the yield of the process in which electrons are released by excited atoms should be on the order of 1.

MALTER's effect was also brought forth to explain the cathode emission, by which the oxide layers obtained by reaction of the electrode gas on the cathode surface would be cahrged by positive ions and would produce electric fields on the order of 10^9 V/m, which is enough to promote the electronic emission.

Modern theories use systems of equations to try to describe interdependent processes in the cathode region and at the cathode.

HOLMES (14) proposes an analysis of the problem. His results give a correct order of magnitude of the various parameters such as the current density, the cathode drop and the electric field, but   /16 in regard to the cathode temperature, he comes to much higher values than those observed - BADARU - POPESCU (1), Von ENGEL (3).

Furthermore, the continuity of the current opposite the cathode necessitates ion production. Ions may be produced either by thermal ionization, or by gas ionization due to shocks with electrons accelerated by the cathode drop.

2.3.2 - Anode Region

The anode region has features which are similar to the cathode region, such as contraction near the electrode and the potential

drop due to the space charge.

Few studies were conducted on the anode, because it is considered to play only a passive role, limited to collecting electrons without any emission process. This poses the problem of knowing why the anode region has a higher current density (contraction at anode) than that of the positive column, despite the fact that no emission is necessary.

The current continuity opposite the anode poses the problem of knowing how ions are produced. A strong electric field may produce them by accelerating electrons through a layer without collisions which approach the anode and ionize the gas.

This possibility was proposed by BEZ and HOCKER (15). They /17 divided the anode region into three areas: the first is a transition are where there is a transition from the positive neutral column of one side to a negative space charge region on the other side. The second area is an acceleration area where electrons doe not undergo collisions but increase in energy before arriving at the last area where they make ionizing shocks.

One of the problems of this theory lies in the fact that the author does not account for potential inelastic collisions in the acceleration area.

2.3.3 - Plasma Jets

Another aspect of the arc, which would be an effect of the mechanisms described, is the initiation of the electrode in the form of steam with a directed material velocity, especially for high currents. The origin of these jets is probably due to:

1) either a vaporization or pulverization of the electrodes,
2) electromagnetic effects on particles charged near the electrodes,
3) or to chemical reactions with gas production.

The problem was handled in a general manner by ECKER (10) using hydrodynamic transport equations.

These plasma jets are originally forces exerted by the arc on the electrodes and which were observed and measured by several authors.

2.4   EROSION CAUSED BY AN ARC   /19

Erosion is a loss of electrode matter which may be in the form of ions, substances (steam), particles (liquid drops, aggregates, solids).

This is a phenomenon where factors are involved (or parameters) which we will try to describe as well as their influences. Then, we will establish an energy balance on each electrode and examine the various erosion models using the terms in this analysis.

2.4.1 - Erosion Factors

One of the important parameters is the pressure of ambient gas. In figure 5, according to KIMBLIN (16), we show that the mass loss of the cathode depends on the pressure. This is probably due to a redeposition of the metallic steam and of the ions because of collisions with substances.

The same figure shows us the influence of the nature of the surrounding gas: monoatomic or diatomic gas, chemical activity. We see that erosion is greater for lighter ambient gases.

Another parameter involved is the current, as we can see in fig- /20 ure 6 according to KIMBLIN (16). The steady erosion in the case of arcs in the vacuum would be due to the multiplication of the number /21 of spots with the current. Each spot would produce a constant erosion rate. As of 10KA, there is only one large spot which would then produce an intense evaporation.
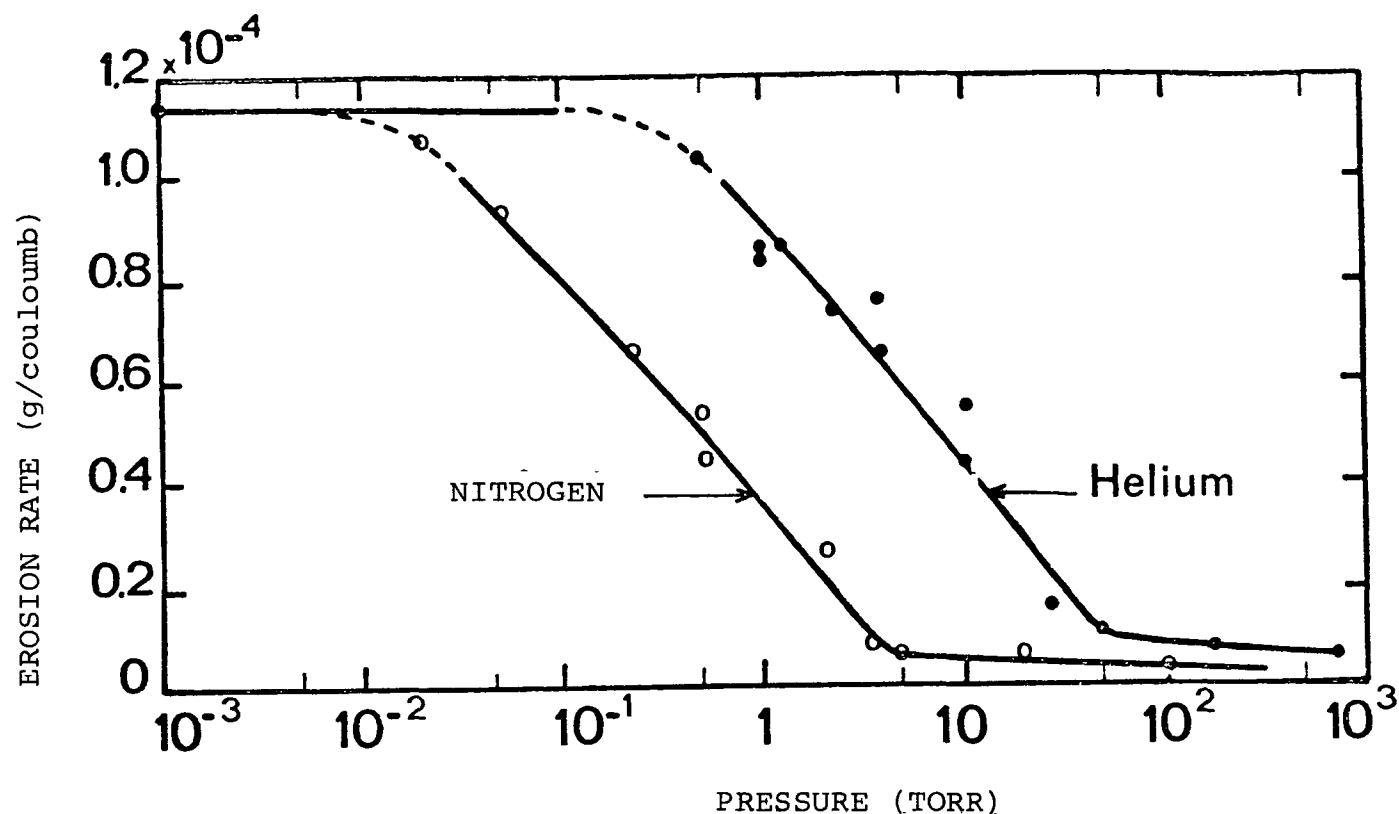
14

Figure 5 - Variations in the erosion rate measurements of a copper cathode as a function of the surrounding gas pressure. Arc current: 100A.
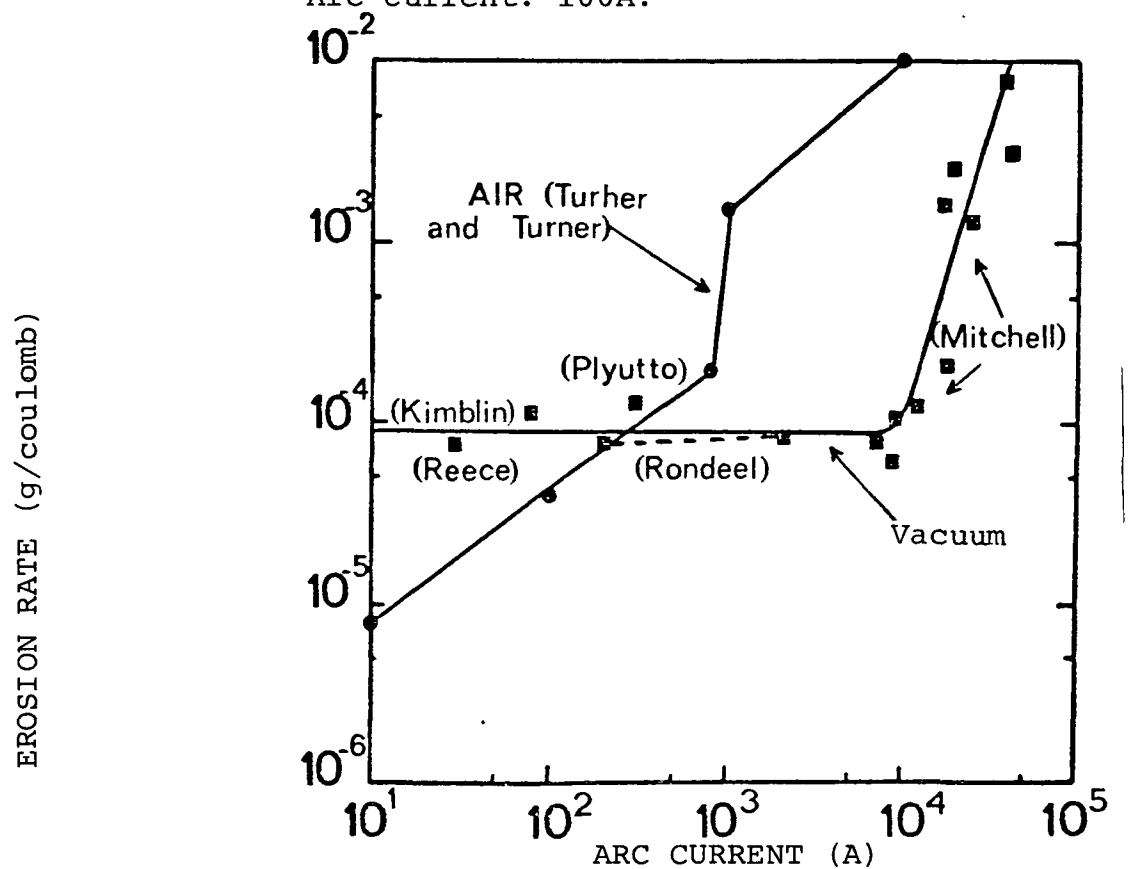

Figure 6 - Copper electrode erosion rate as a function of the arc current. Cathode erosion in a vacuum. Total electrode erosion in air.

15

Furthermore, KIMLIN (17) shows that a cathode's erosion depends on the thermal properties of the material it is made of, such as the boiling point, the latent vaporization heat, etc. GUILE (18) showed that the nature of the cathode surface plays a role in its eroson. When the oxide layer changes from 2 to 10 nm, the erosion changes: from a evaporation followed by condensation, it becomes microexplosive with an initiation of melted globules.

One approach in understanding the erosion mechanisms is establishing an energy balance on each electrode.

2.4.2 - Energy Balance

2.4.2.1 - CATHODE: among the energy sources, we may mention:

a) The thermal energy of ions plus the kinetic energy obtained when passing through a cathode drop. In order to put this source in numbers, it is necessary to know the ionic current density and the cathode drop. We may mention the work of von ENGEL (3), KESAEV (4), GRAKOV (20) in regard to the cathode drop which depends on the nature of the material.

b) The ion neutralization energy. Since one cathode electron /22 is needed to neutralize an ion, the available energy is therefore $e(V_i - \Phi)$. eV_i is the ionization energy of the atom and $e\Phi$ the cathode discharge energy.

c) The conduction heat from the column due to neutral and excited atoms.

d) The radiation energy of the column to the cathode if the column is shorter than the cathode its contribution may be great.

e) The chemical reactions on the cathode surface. SZABO (21) demonstrated a decline in the electrode temperature and reactivity of the material, due to the current.

f) The heat produced by Joule's effect when the current passes through the cathode spot in the material. Calculations of this effect include those of RICH (22). Erosion due to Joule's effect was treated by GUILE and HITCHCOK (24).

The energy losses at the cathode are:

a) the energy from the electron emitted (eΦ). This cooling effect was calculated by LEE (24).

b) The energy required for vaporizing the cathode material.

c) The energy dissipated at the time of explosions and departures of micro-particles.

d) Radiation from cathode spots.

e) The energy lost to dissociate the molecular gases which surround the electrodes (high pressure arcs).

f) The energy lost by conduction through the electrode.   /23

g) The heat lost by convection or due to transfers with the atmosphere.

h) Heating and melting energy in a transient state or mobile arc.

2.4.2.2 - ANODE: The Energy Supplied is:

a) The potential electron energy e due to the entry of e into the anode material.

b) The electron heat energy which is $\frac{3}{2}$ KT.

c) The energy supplied by neutral and excited atoms, the recombination of dissociated gases on the surface. The conduction and

17

radiation heat of the column, the chemical reactions on the electrode, the heat due to Joule's effect when the current passes into the anode material.

The energy losses are:

a) The energy lost by vaporization of the electrode. COBINE (25), in his analysis of phenomena at the electrodes with strong and short currents, showed that virtually all the power injected at the anode was dissipated by evaporation.

b) The energy lost by the departure of large particles.

c) The energy lost by radiation of the anode spots.

d) The energy lost by dissociation of the molecular gases on the hot surface.

e) The heat lost due to conduction through the electrode.   /24

f) The heat lost due to convection and conduction with the atmosphere.

2.4.3 - Erosion Models

One of the models proposed by GRAY (26), which tries to explain the droplet formation observed on the electrodes, is the following:

During the arc period, the force caused by ion or electronic bombardment of electrodes is exerted over a melting crater. When the arc in this crater is interrupted, the surface voltage is exerted over the melted part of the crater. A drop is formed and freed. Calculations of the various forces would explain the diameter of the drops observed.

Another approach in trying to explain the erosion phenomenon

is that of GUILE (18). He explains that the oxides on the cathode surface should be responsible for the erosion. Depending on the thickness of the oxide layer, the manner in which the material changes is lost changes:

-If the thickness of the oxide layer is on the order of 2×10^{-9} m, an electric field due to positive ions deposited on its surface may cause an electronic emission and evaporation of the metal without formation of a crater.

-If the oxide layer is on the order of 10×10^{-9} m or more, the conductor filaments due to a phase change in the oxide. A current increase transmitted through these filaments would produce a Joule's effect anda rupture of these filaments with explosion and formation /25 of craters. The globules produced by these explosions should be of the same dimension as that of the craters.

One of the last models proposed by DROUET (27), based on the MITTERAUER's Work (28), to account for the formation of craters on the electrode based on the measurement of the current distribution at the cathode.

He shows that with a 700A arc, the micropoints which become craters have a lifespan of 1 μs, with individual currents of 0.6A and a current density of 10^{14}A/m^2.

CHAPTER 3 - STUDY OF ELECTRODE MASS LOSS DUE TO THE INTENSITY
         OF AN EMISSION LINE   /26

3.1 ASSUMPTIONS

The measurement of the mass loss of electrodes subjected to the effects of an electric arc, by measuring the intensity of an emission line of the electrode material, is based on several assumptions:

a) The optical transparency of plasma, i.e. any photon emitted

by the medium will leave it without being absorbed.

b) The existence of a local thermodynamic equilibrium (E.T.L.), which makes it possible to find the total number of atoms with an N line.

c) The ratio between the total number of N atoms and the electrode mass loss per second.

In the following sections we will discuss these three assumptions.

3.2 - OPTICAL TRANSPARENCY OF THE PLASMA

The optical transparency of the plasma with the wavelength under consideration was assured by two means:

a) Selecting lines whose lower level j is neither the fundamental nor a metastable level, because they are generally self-absorbed;
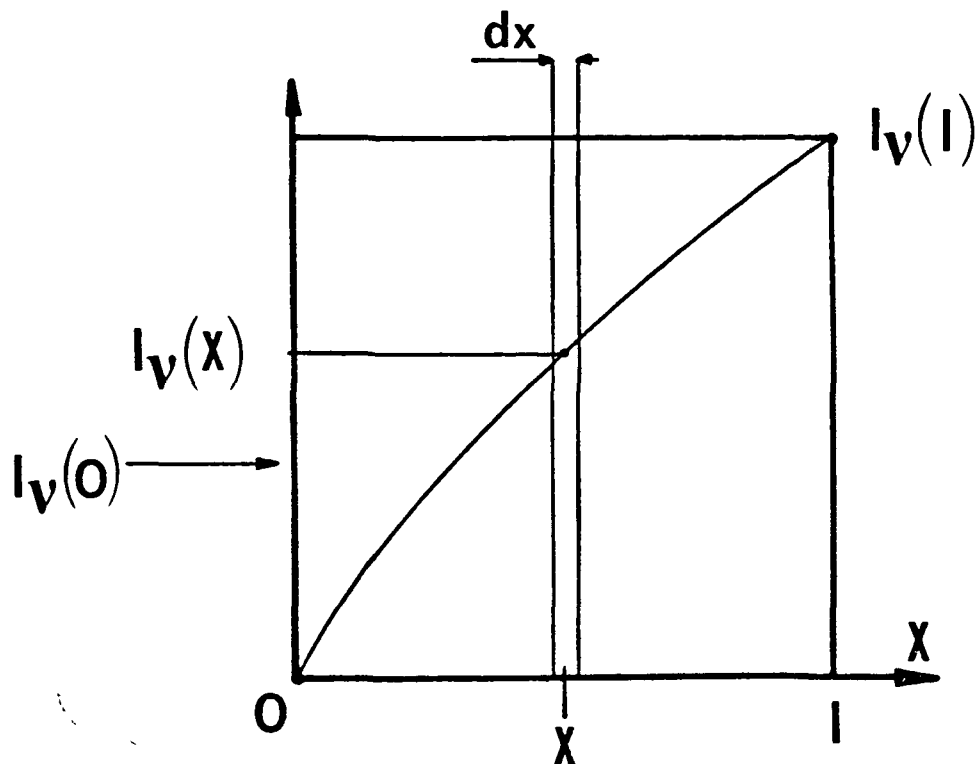
b) once the lines are selected, an experimental method is used to check the transparency. The principle is the following:

Let us consider a plasma of width 1, with the light propagating toward the observer along direction Ox. Given $I_v(x)$ the intensity emitted at frequency v and at point x, K' (v,x) the absorption coefficient and $\varepsilon_v(x)$ the plasma emission coefficient. The variation of $dI_v(x)$ over a distance dx is equal to the increment $\varepsilon_v(x)dx$ less the absorption K' $(v,x)I_v(x)dx$:

$$\frac{dI_v(x)}{dx} = \varepsilon_v(x) - K'(v,x)I_v(x) \qquad (1)$$

which has the following solution:

$$I_v(l) = I_v(0)exp[-\int_0^l K'(v,x)dx] + \int_0^l \varepsilon_v(x)exp[-\int_x^l K'(v,x)dx]dx \qquad (2)$$

If there is a light intensity $I_\nu(0)$ coming from the outside, it is attenuated by an $\exp[-\int_0^l K'(\nu,x)dx]$ factor.

If one considers $\varepsilon_\nu(x)$ and $K'(\nu,x)$ independent of position x and $I_\nu(0) = 0$ equation (2) becomes:

$$I_\nu(l) = \frac{\varepsilon_\nu}{K'(\nu)}\left[1 - \exp\{-K'(\nu)l\}\right] \qquad (3)$$

Let's place a mirror behind the plasma and a monochromator in the observer's place to isolate a spectral band $V_2 - V_1$. Given R the ratio between the itensity I_R measured with the mirror and I the intensity without mirror, then:

$$R = \frac{I_R}{I} \qquad (4)$$

Given the width of the slits used, we have:

$$I = \int_{v_1}^{v_2} I_v(l)\,dv \qquad (5) \qquad \text{and} \qquad I_R = \int_{v_1}^{v_2} I_v(l)\,dv + r\int_{v_1}^{v_2} I_v(l)\exp[-K'(v)l]\,dv \qquad (6)$$

r is the reflection factor of the optical system.

If we place equations (3) (5) and (6) in (4) and expand the exponential term, we obtain:

$$[3r + 1 - R]\int_{v_1}^{v_2} I_v(l)\,dv = 2r\int_{v_1}^{v_2} \varepsilon_v l\,dv - \frac{2}{3}r\int_{v_1}^{v_2} \varepsilon_v l\,[K'(v)l]^2\,dv + \cdots \qquad (7)$$

If the line is optically thin $K'(v)| \to 0$ and we have:

$$\int_{v_1}^{v_2} \varepsilon_v l\,dv = \frac{1}{2r}[3r + 1 - R]\int_{v_1}^{v_2} I_v(l)\,dv \qquad (8)$$

This shows us that it is necessary to multiply the measured intensity $\int I_v(l)\,dv$ by a corrective factor to include the optical thickness of plasma because the integral of the left side is the intensity of an optically thin plasma.

The reflection factor of the optical system was determined using the continuous background close to the lines used, considered to be optically thin. This was suggested by VUJNOVIC (30).

3.3 - LOCAL THERMODYNAMIC EQUILIBRIUM

The existence of E.T.L. in the arc was and continues to be a subject of dispute because it conditions and validates the temperature and electronic density measurements performed by spectroscopic methods.

According to L. MARTON (31), two conditions must be fulfilled

obtain E.T.L. in an arc:

a) the energy gained per second by the electrons in the electric filed E of the column is equal to the energy lost by collisions with heavy particles:

$$v_d = \mu . E \qquad (10)$$

$$eEv_d = \frac{3}{2} k(T_e - T_g) \frac{2m_e \langle v_e \rangle}{m\lambda} \qquad (9) \qquad \text{where}$$

$$\langle v_e \rangle = \sqrt{\frac{8kT_e}{\pi m_e}} \qquad (11)$$

v_d is the mean electron driving velocity, $\frac{3}{2}(T_e - T_g)$ the energy surplus of electrons versus heavy particles $\frac{2m_e}{m}$ is the energy fraction transferred by shock, $\frac{\langle v_e \rangle}{\lambda}$ is the collision frequency with the mean electron velocity $\langle v_e \rangle$ and λ the mean free electron path from which the condition is derived for the temperature difference at equilibrium:

$$\frac{T_e - T_g}{T_e} = \frac{\pi m}{24 m_e} \left\{ \frac{Ee\lambda}{kT_e} \right\}^2 \ll 1 \qquad (12) \qquad\qquad \mu_e = \frac{e\lambda}{m_e \langle v_e \rangle} \qquad (13)$$

This condition may be fulfilled if E and λ are small, which is /31 the case for the arcs in the air which we studied where E is less than 70V/cm and λ on the order of 10^{-5}cm. A value of about 10^{-2} is obtained for $\frac{T_e - T_g}{T_e}$.

b) The collision processes play a more important role than the radiative processes. Since electrons are involved in the excitation and ionization processes, a minimum electron density is necessary to assure an adequate number of collisions. It was calculated by GRIEM (32), in the case of hydrogen:

$$N_e \geqq 9 \cdot 10^{17} \left\{ \frac{kT}{E_H} \right\}^{\frac{1}{2}} \left\{ \frac{E_2}{E_H} \right\}^3 \; [cm^{-3}] \qquad\qquad (14)$$

where E_H is the ionization energy of the hydrogen atom and E_2 the excitation energy of level 2 of the atom, corresponding to the resonance line.

The preceding equation is valid for plasmas which are optically thin. In the case of arcs where the resonance lines are often self-absorbed, the radiative de-energizations of the first excited level are counterbalanced by radiative excitations of the fundamental level.

The other radiative de-energizations to the fundamental, from higher levels, are not counterbalanced by radiative exciations (they are not self-absorbed). An examination of the transition probabiliites shows that this process is ten times less probable than in the case of resonance lines. The condition for N_e, therefore, will be less severe and we may express:

$$N_e \geq 10^{17} \left\{ \frac{kT}{E_H} \right\}^{\frac{1}{2}} \left\{ \frac{E_2}{E_H} \right\}^3 \; [cm^{-3}] \qquad\qquad (15)$$

For temperatures of about 5000-60000°K and for an excitation energy E_2 = 3.78eV (corresponding to the first excited eleve of the Cu atom), we obtain an electronic density $N_e \geq 4.2 \times 10^{14} cm^{-3}$. I. MIYACHI (33) estimates a value of $N_e = 10^{15} cm^{-3}$ in an arc with copper electrodes and for a 5A current in the air, based on SAHA's law.

3.3.1 - Temperature Variation

As far as we can define it, the temperature of substances in an arc is an important parameter and its determination was the subject of numerous experimental studies, but most of these were performed on arcs stabilized by walls or long arcs, where it is mainly the surrounding gas which is excited and ionized.

The temperature variation was studied as a function of the current using the method of the relative line intensity ratio of the same element.

Based on relationship (2), we may express the intensity ratio /33
of two lines belonging to the same atomic species and in the same ionization state:

$$\frac{I_1}{I_2} = \frac{A_1 g_1 \lambda_2}{A_2 g_2 \lambda_1} \exp\left\{-\frac{E_1 - E_2}{kT}\right\} \tag{16}$$

with $\lambda = \frac{c}{\nu}$

If we examine this expression, we see that it is possible to determine the temperature if we measure the intensities I_1 and I_2 and we know the probabilities of transition A_1 and A_2.

If we derive expression (16), we obtain:

$$\frac{\Delta\left[\frac{I_1}{I_2}\right]}{\left[\frac{I_1}{I_2}\right]} = \frac{\Delta T (E_1 - E_2)}{T \quad kT} \tag{17}$$

In order for a line intensity ratio to be sensitive to the temperature, we must select these lines with a deviation between the departure levels E_1 and E_2 which is as large as possible. Unfortunately, this condition is difficult to fulfill for metallic atoms in general because the first excited level is already near half of the ionization potential of the atom and the radiative transitions to the fundamental level are highy self-absorbed.

It is not necessary to determine the absolute temperature value /34 but it is simply necessary to know its law of variation as a function of the current. The I_1/I_2 ratio was studied as a function of the current for the three metals used.

3.4 - RATIO BETWEEN THE EROSION RATE AND THE INTENSITY OF A SPECTRAL LINE

The light intensity of an emission line expressed in erg $sec^{-1} cm^{-2}$

os

steradian^{-1} is:

$$I_{ij} = \frac{1}{4\pi} nlA_{ij}h\nu_{ij} \frac{g_i}{U(T)} \exp\left(-\frac{E_i}{KT}\right) \qquad (18)$$

where A_{ij} (sec^{-1}) is the probability of transition of level 1 to level j, n(cm^{-3}) is the total atom concentration with a line, h is PLANCK's constant, ν_{ij} the radiation frequency, 1 the thickness of the transmitting plasma layer, g_i the statistical weight of level i, U(T) the partition function the values of which are calculated in reference (29), E_i the energy of the higher transition level, K BOLTZMANN's constant and T the temperature.

If the temperature remains contant and if the medium is optically thin, we may express equation (18) in the following manner:

$$I_{im} = K_{ij} N \qquad (19)$$

with N = nls, s is the surface of the emissive layer, K_{ij} is a constant whichcontains all factors assumed to be knwon for the transition ij under consideration as well as the geometric para- /35 meters of the measuring system and N the total number of atoms with a line. We assume that the total number of atoms with line N is proportional to the mass loss of the electrode per second, i.e.:

$$\frac{dm}{dt} = \frac{\gamma}{\tau} N \qquad (20)$$

where γ is a constant and τ, which has a time dimension, the time of its presence in an atom, torn from the electrode, in the arc. By combining equations (19) and (20) we obtain:

$$I_{ij} = cte \frac{dm}{dt} \qquad (21)$$

Equation (21) may be used and compared to the electrode mass loss whichvis determined by weighing.

The intensity of each line is measured using a photomultiplier

(P.M.) placed behind a monochromater (M.C.) which helps us to separate the different lines. It is evident that the line selection is also a function of the M.C. separator ability, because the lines must be separated enough to avoid superpositions.

The P.M. delivers a $Q_{PM}(t)$ charge proportional to the light quantity Φ $(i_{PM}=\alpha\Phi)$. The electric chrage is tored in a capacitor for awhile. The charge of capacity C in the capacitor is proportional to the voltage V at its terminals:

$$V = \frac{Q_{PM}}{C} \qquad (22) \qquad /36$$

If we integrate for a time interval t, which is clearly longer than the light intensity fluctuation time, we obtain a mean value of I_{ij} which is therefore:

$$\overline{I}_{ij} = \frac{VC}{K' \, \Delta t} \qquad (23)$$

CHAPTER 4 - EXPERIMENTAL STUDY   /37

4.1 - EXPERIMENTAL DEVICE
4.1.1 - Electric Power System

A direct current electric power supply with an output of up to 30A, and a voltage of 300V is connected using a rheostat to the electrode terminals. The Current range covered during this study is 2 to 10A.

We placed a capacitor between the rheostat cursor and the ground to filter the power supply ripples. Calculations show that this ripples are the smallest when the cursor is in the middle of the rheostat.
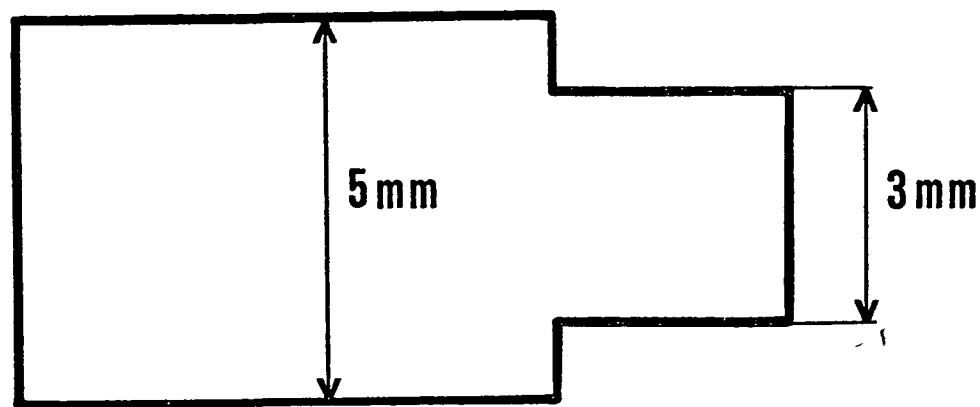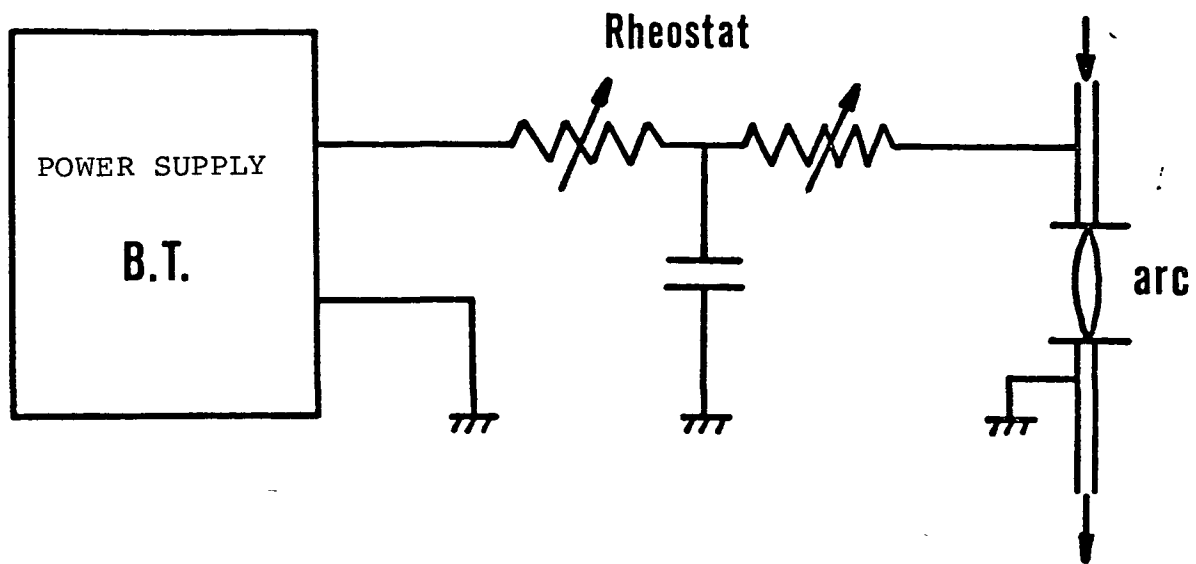
4.1.2 - Electrode Geometry and Support   /38

4.1.2.1 - Electrode Geometry

The electrodes are cylindrical as shown in the figure. The

Rheostat

POWER SUPPLY

B.T.

arc

5mm

3mm

Figure 9 - Electrode Geometry

electrode is clamped by pliers on the side with the largest diameter. The reason for this geometry is to be able to limit the arc movement during the spectroscopic explortaion experiments where the arc is parallel to the input slit of the spectrograph and which we retained thereafter.

The electrodes used during this study are made of copper, silver

or nickel, either in symmetrical (anode and cathode of the same material) or dissymmetrical couples (anode and cathode of different materials).

The currents used are lower than the admissible electrode currents, because the current densities absorbed with Cu, Ag and Ni electrodes vary between 10^3 and $1o^6 A/cm^2$.

4.1.2.2 - Electrode Support

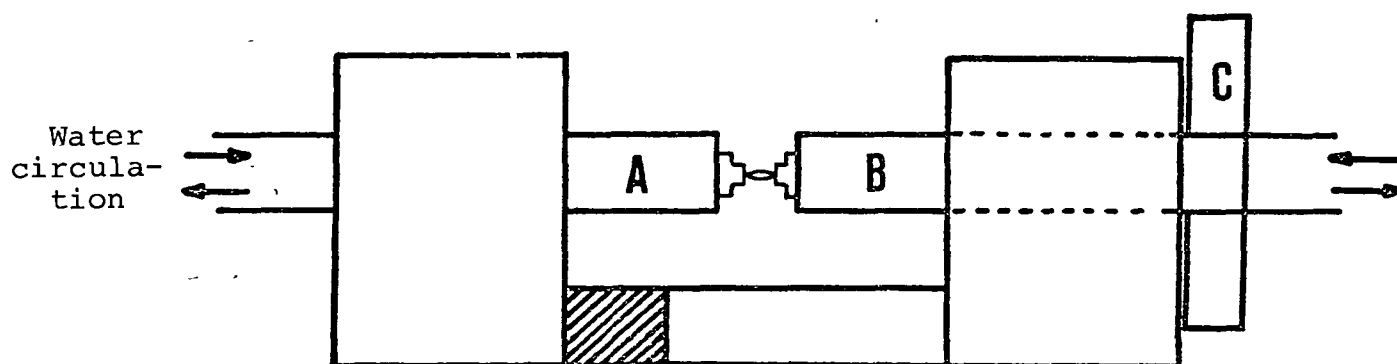The above electrodes are clamped face to face with pliers (as shown in figure 10).

Figure 10 - Diagram of the Electrode Support

Pliers A is attached whereas pliers B moves along an axis via a screw (C) which separates the electrode by one millimeter of a turn. The interelectrode distance during our experimetns was kept at 2 mm.

Water circulates inside the pliers to cool the electrodes.

4.1.3 - Optical Measuring System

4.1.3.1 - System for Measuring the Line Intensity

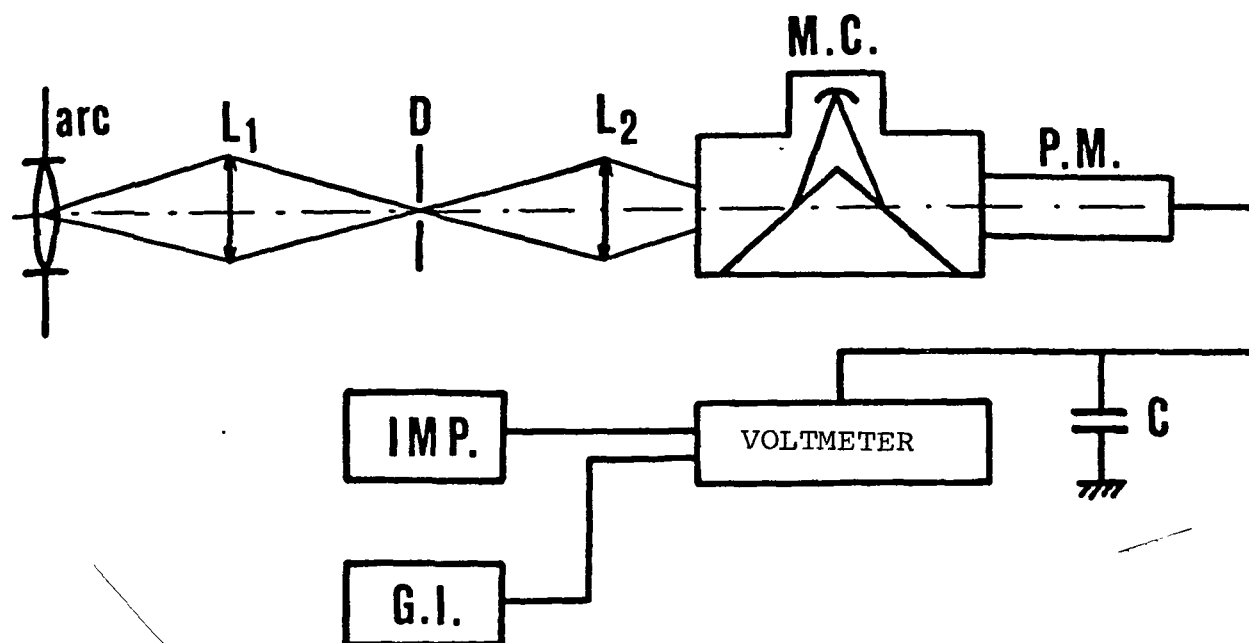The arc is horizontal and perpendicular to the axis of an optical

system (figure 11).

Figure 11 - Diagram of the Line Intensity Measuring System

Lens L_1 form an arc image on diagram D to limit the light received to that leaving the arc column and to remove the regions close to the electrodes and the electrodes themselves which are the center of high thermal graidents and high fields.

The monochromator (M.C.) is placed in such a manner that the image of diaphragm D given by lens L_2 is unfocused to integrate the unhomogeneous emissions of the arc in space. The M.C. used has an opening of F/35 with a concave holographic network (1200 lines/mm) and corrected of astigmatism. The dispersion is linear and is 40Å/mm. The input slit is 0.05 mm whereas the output slit is 0.1 mm to facilitate the adjustment on the selected line. The width of 0.05 mm corresponds to a spectral spread of 2 Å.

30

The photomultiplier (P.M.) placed behind the M.C. is a 14-stage
tube. Its trialcaline photocathode has a spectral response as shown
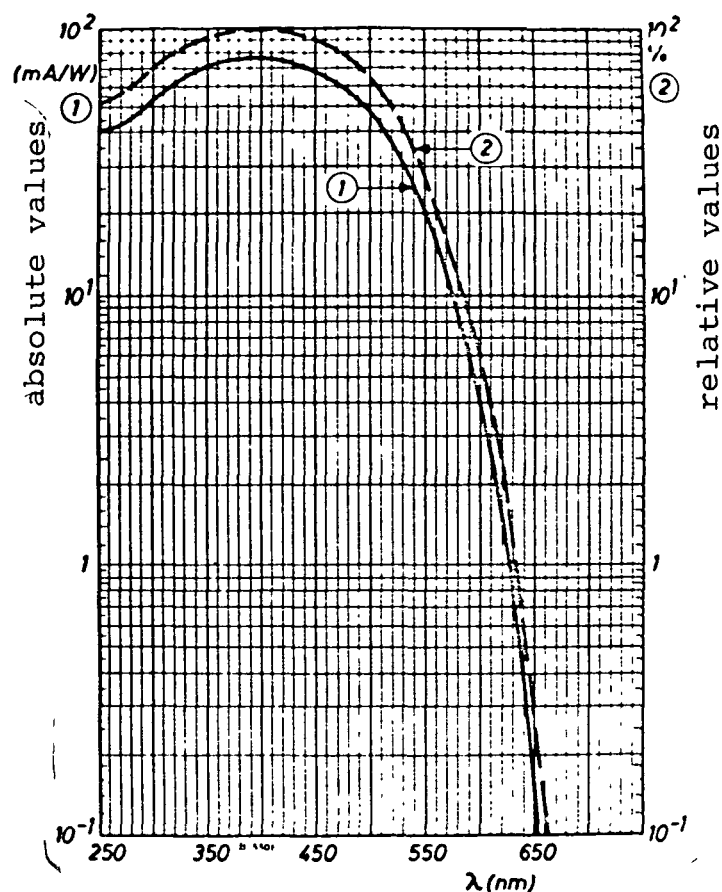in figure 12.

Figure 12 - Spectral Response of the 56 DUVP
Photomultiplier

The high power supply voltage is 1400 V. The P.M., which gives
us a current proportional to the light flux, charges the capacitor
(C) (1μF), the voltage of which is measured using a high impedance
digital voltmeter ($10^{14}\Omega$). The voltmeter is controlled by a periodic
pulse generator and is connected to a ribbon perforator. We thus
controlled the capacitor charge in time.

The same assembly is used for testing the method of measuring   /42
the ground loss due to the intensity of a line, and the method of
measuring the temperature.

When the intensity of an emission line in plasma is measured,
one must make sure that the medium in which the emission is measured
is optically thin. To do this, a simple method consists of having
the plasma crossed by its own radiation using a mirror and measuring
the line intensity in the absence and in the presence of a mirror.
In practice, when the mirror is in place, the intensity should be
twice as great as the intensity measured without a mirror, if the
line is optically think.

To accomplish this, the electric arc is over the optical axis
formed by two lenses L_1 and L_2 with the same focal distance. The
lens L_1 sends a light beam parallel to a cube corner which has the
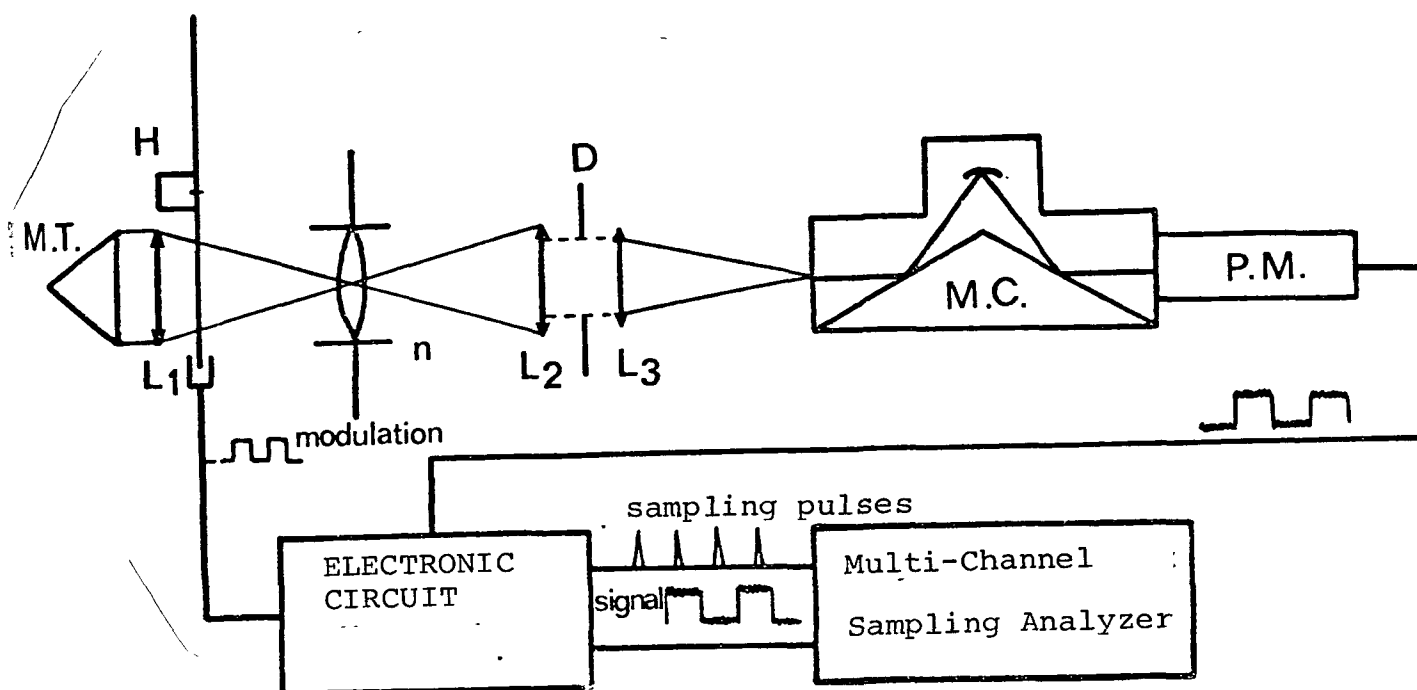property of sending the beam parallel to itself (figure 13).

Figure 13 - Diagram of the Line Optical Transparency Control
              System

31A

The optical system, made up of a lens L_1 and a triple mirror, has a magnifiction of +1. This property was sued to correct the random movement of the arc which makes it impossible to measure using conventional systems with either a spherical mirror or a lens and a flat mirror. These systems have a magnification of -1 and give an inverted image of the arc.

The light H placed beween the lens L_1 and the arc allow us to measure the intensity of a line with or without the reflected beam.

Lens L_3 forms an arc image on the M.C. input slit, the diaphragm D is used to adjust the beam spread.

When the arc is established and the light rotates, the signal produced by P.M. to the oscilloscope is shown on the photo.
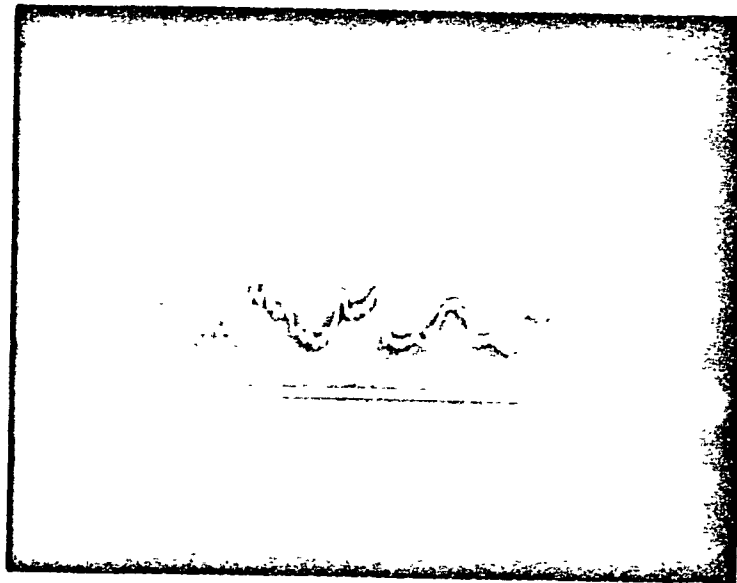

Figure 14 - P.M. Signal Before Electronic Circuit

The height of the lower or upper level of the pulse represents the intensity of the line observed with or without the mirror, respectively. Since the intensities vary in time, we built an electronic circuit (figure 15) which samples the voltage of each level
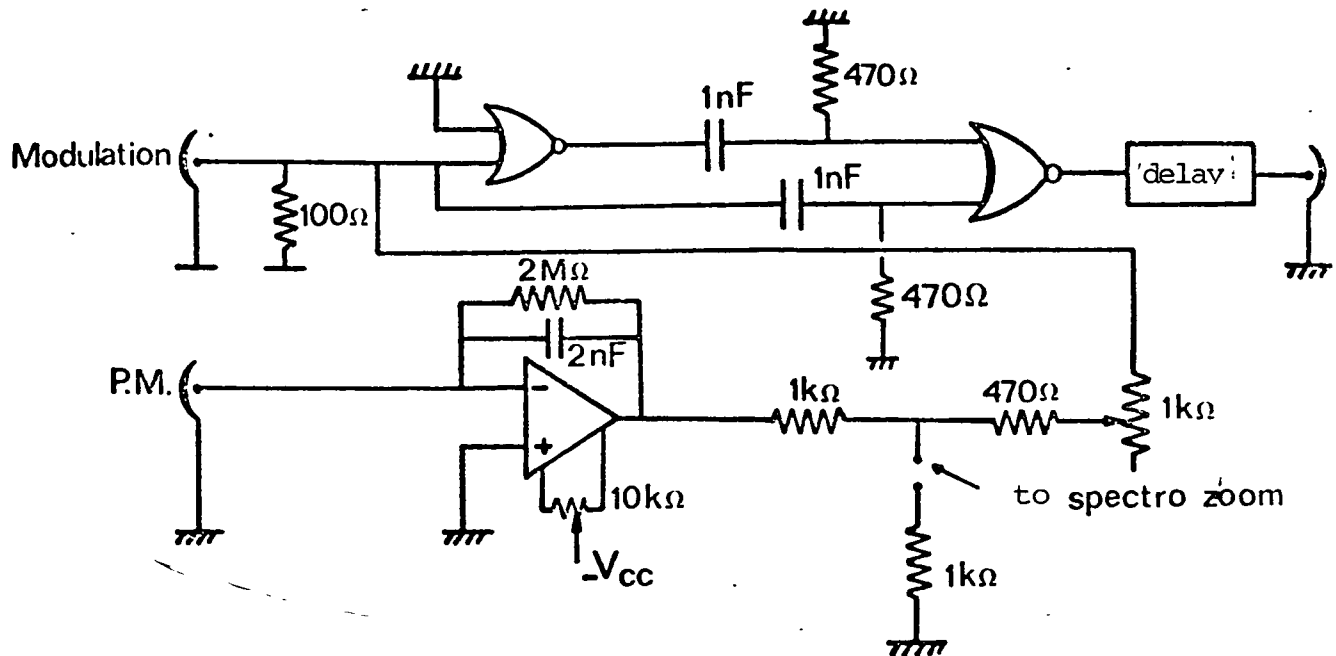
and stores it in memory.

Figure 15 - Electronic Device For Sampling the P.M. Signal

To accomplish this, the modulation signal, associated with light chopper blades passing in front of lens L, is sent into a circuit which gives a delayed enough sampling pulse to control the sampler and to add 2 volts to the upper level of the pulse to stagger the sampled value in memory.

The sampling of the sampler system and associated circuit was /45 accomplished by applying a constant voltage at the input. The sampler, whose input voltage may vary from 0 to 4V ahs a definition of 200 channels, which represents a conversion slope of 20 mV/channel.

The circuit used for staggering the signals at the sampler in-put, reduces the conversion slope to 18mV/Channel in the staggered part of the signal.

The cutting frequency of the light chopper is 125 Hz, which

33

prevents interferences with the frequency of the sector or its harmonics.

4.2 - EXPERIMENTAL PROCEDURE

4.2.1) - Measurement of the Flux Emitted

After the arc is established, the photomultiplier current is integrated for a time which varies with the current (between 30 and 600 seconds). The capacitor charge is measured every 1 or 10 seconds, depending on the current value.

We therefore obtain a series of values for the capacitor charge taken at regular intervals. The equation for the straight line, passing through these points, is obtained using the least squares method, whose slope is proportional to the line intensity.

The line torques used for determining the temperature variations /46 are:

For Ag $4d^{10}5d\ D - 4d^{10}5p\ ^2P^o(5471\text{\AA})$ -- $4d^{10}7S\ ^2S - 4d^{10}5p\ ^2P^o(4476\text{\AA})$

For Ni $3d^8\ 4S5s\ ^5F - 3d^8\ 4s4p\ ^5G^o(4600\text{\AA})$ -- $3d^9\ 4p\ ^1P^o - 3d^{10}\ ^1S\ (5476\text{\AA})$

For Cu $3d^{10}5d\ ^2D - 3d^{10}4p\ ^2P^o\ (4022\text{\AA})$ -- $3d^{10}4d\ ^2D - 3d^{10}4p\ ^2P^o\ (5153\text{\AA})$

The lines used for measuring the mass loss are:

$$3d^9\ 4s\ 5S\ ^4D - 3d^9 4s\ 4p\ ^4D\ (5292\text{\AA}) \quad \text{for Cu,}$$

$$4d^{10}8s\ ^2S - 4d^{10}5p\ ^2P^o\ (3981\text{\AA}) \quad \text{for Ag,}$$

$$3d^5\ 4s4p\ ^1F^o - 3d^5\ 4s^2\ ^1D\ (4520\text{\AA}) \quad \text{for Ni.}$$

In order for the photomultiplier to supply an anodic current proportional to the incident light flux, the voltages between each stage must remain constant. The supply bridge is calculated to make the voltage drop causeed by the passing current negligeable. Now one must make sure that the voltage at the capacitor (C) terminals does not influence the anodie current of the photomultiplier. To accomplish this, the anode voltage -last dynode - must remain

34

above 50 V. The voltage applied to the last stage is now 100 V.
The capacitor voltage is therefore limited to 50 V.

Now that we have found that the anode current of the photomulti-
plier, and therefore the flux received, varied by 2 to 3 orders of
magnitude when the arc current increased from 2 to 10 A, we checked
whether the linearity between the flux and anode current of the photo-
multiplier is observed within a 10% range, in our assembly.

4.2.2) - Checking the Plasma Transparency   /47

In figure 16, the x-axis represents the light intensity and
the y-axis axis the number of samples. Since the sampling frequency is
constant, each value of the light intensity is represented by a
number of smaples which is proportional to time. The mean temporal
value of the intensity coincides with the position of the center of
gravity in the figure.

This determination was performed for all lines used and for
current values from 2 to 10 A as well as for the continuous back-
ground adjacent to each line..

4.2.3) - Determination of the Electrode Mass Loss   /48

The detachable part of the electrodes is marked and weighed
first using a scale with a sensitivity of 0.1 mg. The electrodes
are placed in contact with each other and the current is circulated.
The arc is established by separation up to a distance of 2 mm and
is left operating for 30 to 1000 seconds (by measuring with a chron-
ometer), based on the current value, to be able to obtain a mass
loss detectable on the scale. For strong currents, and to avoid
welding, the arc is established with a current of 2A and after the
electrodes are separated by 2 mm, the current is increased. After
the arc goes off, the cooled electrodes are cleaned with a 50%
acetic acid solution in an ultransic tank and weighed again to

Figure 16

Amplitude distribution
of each signal level.

determine the actual amount of lost metal or metal transformed
into oxide.

CHAPTER 5 - LIGHT EROSION RELATIONSHIP - RESULTS AND DISCUSSION

5.1 - INTRODUCTION

In this chapter we will analyze the results concerning the optical
transparency and temperature of arc plasma. After the introduction
and discussion of results of the erosion rates measured with the
microscale, we will present the results concerning the relationship
between the erosion rates and line intensities.

5.2 - OPTICAL TRANSPARENCY OF PLASMA

One of the contributions to the absorption factor of the the
continuous background are the molecular band systems of air. GIL-
MORE (37) showed that the air absorption coefficient, at about 6000°K
and within the wavelength ranges used, is on the order of 10^{-2}cm^{-1},
and therefore very low.

Another contribution to the continuous background are the attached-
free and free-free transitions. According to ZEL'DOVICH (38), the
absorption due to bremstrahlung (free-free transition), and the absorp-
tion of a photon accompanied by the transition of an electron to con-
tinuum have very little effects in our experimental conditions. The
calibration of the optical system by a continuous background, assumed
to be optically thin, gave values of the R ratio which are on the
order of 1.8 - 1.6. The transmission factor calculated for the opti-
cal mirror system triples and the lens L is about 97%, because these /50
elements are treated with antireflecting layers. The deviation be-
tween the measured value and the calculated value is probably due to
a light refraction near the edges of the arc. The incidence of the
reflected beam is no longer perpendicular to these areas where there
is an index gradient of air due to the temperature gradient.

38

a) - In regard to silver, the coefficients for which the line intensities must be multiplied to include absorption is, according to our experiments:

For line 3.981Å   1.026 to 2 A and 1.03 to 10A

For line 4.476   1.018 to 2 A and 1.028 to 10Z

b) - For nickel, these factors are:

For line 4.520A   1.021 to 2 A and 1.057 to 10 A

For line 5.476   1.147 to 2 A and 1.26 to 10 A

c) - In the case of copper, these factors are:

For line 5.292Å   1.073 to 2 A and 1.13 to 10 A

For line 5.153Å   1.13 to 2 A and 1.179 to 5.3 A

For the latter line, at 10 A, the absorption is so large that the theory elaborated in chapter 3 for calculating this coefficient is no longer valid. In the case of line 5.105, whose supply level is a metastable level, this coefficient is 2A, for higher currents, the absorption is very large.

A measurement was performed for line 3.274Å (copper resonance   /51 line), the ratio R gives a value of 1 for 2A, i.e. the line is highly absorbed as described in chapter 3.

5.3 - VARIATION OF THE PLASMA TEMPERATURE

The coefficients obtained in the preceding sections help us to determine the variation of the intensity ratio of two lines as a function of the current, based on absorption.

The value of the ratio is shown in figure 17 for the three metals studi-d: in the case of nickel and silver, this ratio is constant. As the line 5.105Å is highly absorbed, we use the couple 4.022Å and 5.153Å. The inaccuracy is higher because the energy deviation between the starting levels is low (about 0.7 eV).
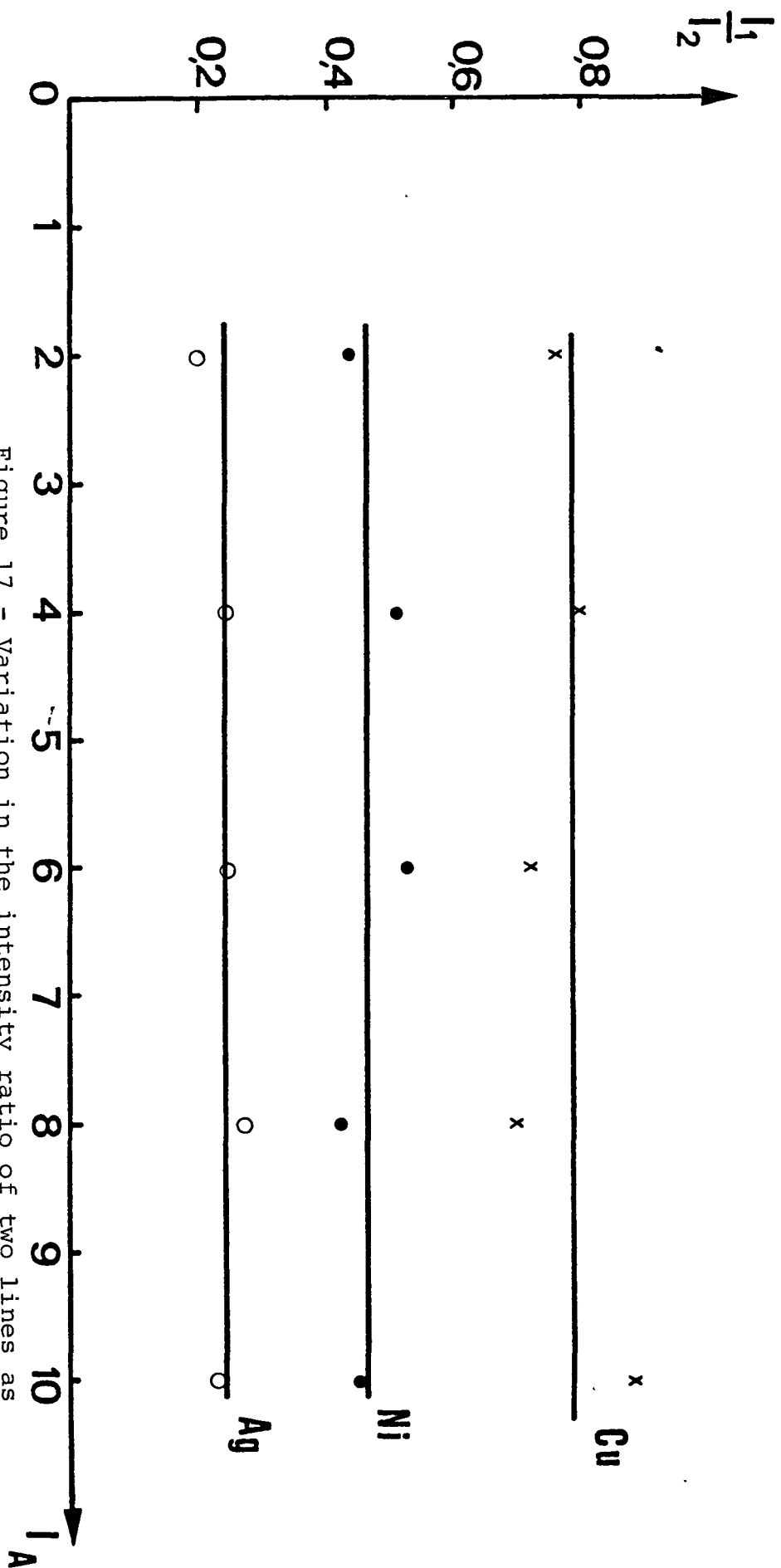
Figure 17 - Variation in the intensity ratio of two lines as a function of the current.

By referring to chapter 3, we used expression (18) in which the
temperature is considered to be constant.

5.4 ELECTRODE MASS LOSS MEASURED WITH A MICROSCALE

Our experiments were performed with silver, copper and nickel
electrodes using symmetrical couples, i.e. anode and cathode
of the same metal as well as disymmetrical couples: anode and cathode
in different metals.

The results show the erosion rate of the electrode, in grams
per second, as a function of the arc current. The curves shown are
based on the polarity and nature of the electrode.

5.4.1 - Results   /53
5.4.1.1 - Cathode

a) Case of Symmetrical Couples

Figure 18 shows the cathode erosion rate when the anode is in
the same material as that of the cathode.

b) Case of Dissymmetrical Couples

Figure 19 shows the erosion rate of a nickel cathode when the
anode is made of silver, cooper or nickel. The mass loss in these
conditions is virutally the same in the three cases.

Figures 20 and 21 show the erosion rate of a cooper and silver
cathode in the same conditions as in figure 19. In virtually all
cases, the erosion rate increases with the current.

5.4.1.2 - Anode
a) Case of Symmetrical Couples

Figure 22 shows the erosion rate of the anode when the cathode
is made of the same material.

41

b) Case of Dissymmetrical Couples. Fiugres 23, 24 and 25 show the anode erosion rate for various cathode materials. The erosion rate of a silver anode is very low when the cathode is in nickel.

5.4.2 - Discussion
5.4.2.1 - Cathodes
a) Case of Symmetrical Couples

One of our assumptions is that the mass loss is proportional to the arc operating time, for a given current. This assumption is genearlly adopted by most authors (KIMLIN (16), TURNER and TURNER (34). It is disputed by GUILE (35) who found that the electrode erosion rate for rotary arcs under a magnetic field is proportinatl to the square root of time. In constrast to arcs in a vacuum, where one finds erosion in grams per coulomb up to currents of 10,000 A, electrode erosion (always expressed in g/C at atmospheric pressures) is an increasing function of the current. Our results for copper agree with those of TURNER and TURNER.

The erosion rates seem to indicate that the thermal conductivity of the material plays a role, because they are ordered according to the thermal conductivity value of each material, i.e. a low conductivity would correspond to a high erosion rate.

	Ni	Cu	Ag
Thermal conductivity in Watt $cm^{-1}\,°K^{-1}$	0.94	4.03	4.29

BUCHET's conclusions (36) on the energy balances of electrodes are along the same lines of thinking because they show that the temperature on one point of an electrode depends on the material used.

Another result of this work is that the total energy expended in the arc depends on the type of metallic steam of the anode. This modifies the conductivity of the column ref. (39) and influences the energy blance at the electrodes, particularly at the cathode.
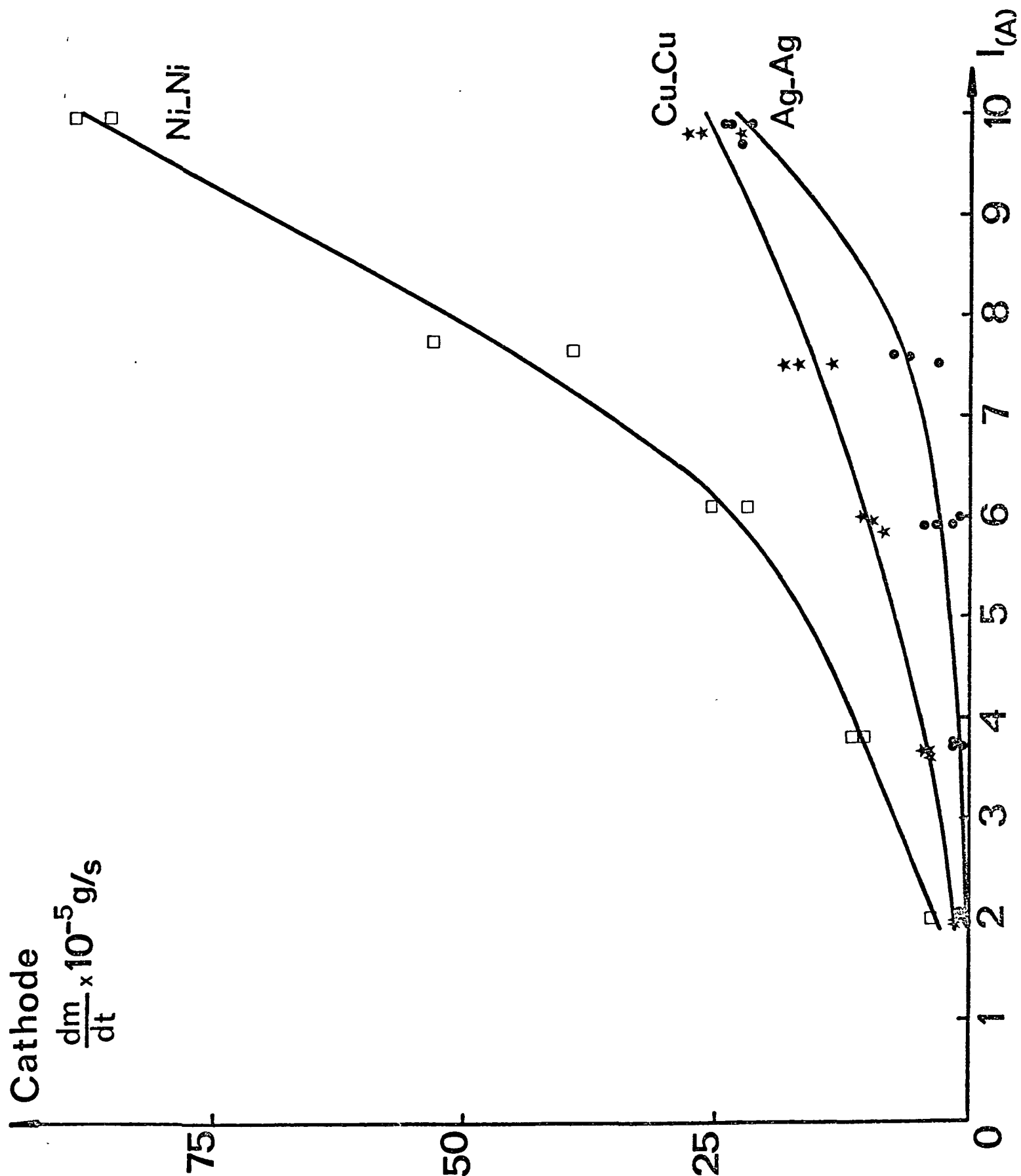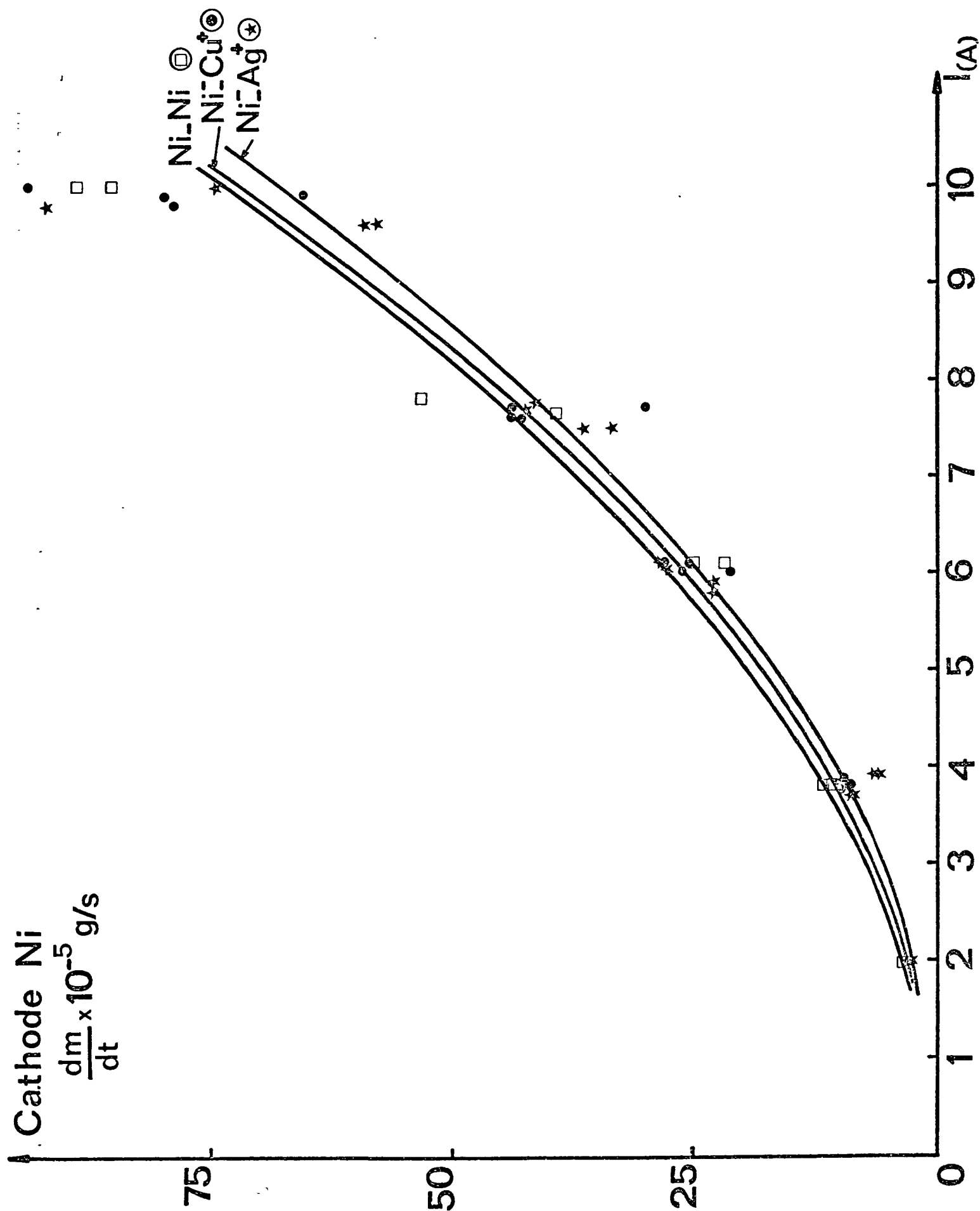
Figure 18 - Symmetrical couples. Cathode erosion rate as a function of the arc current.

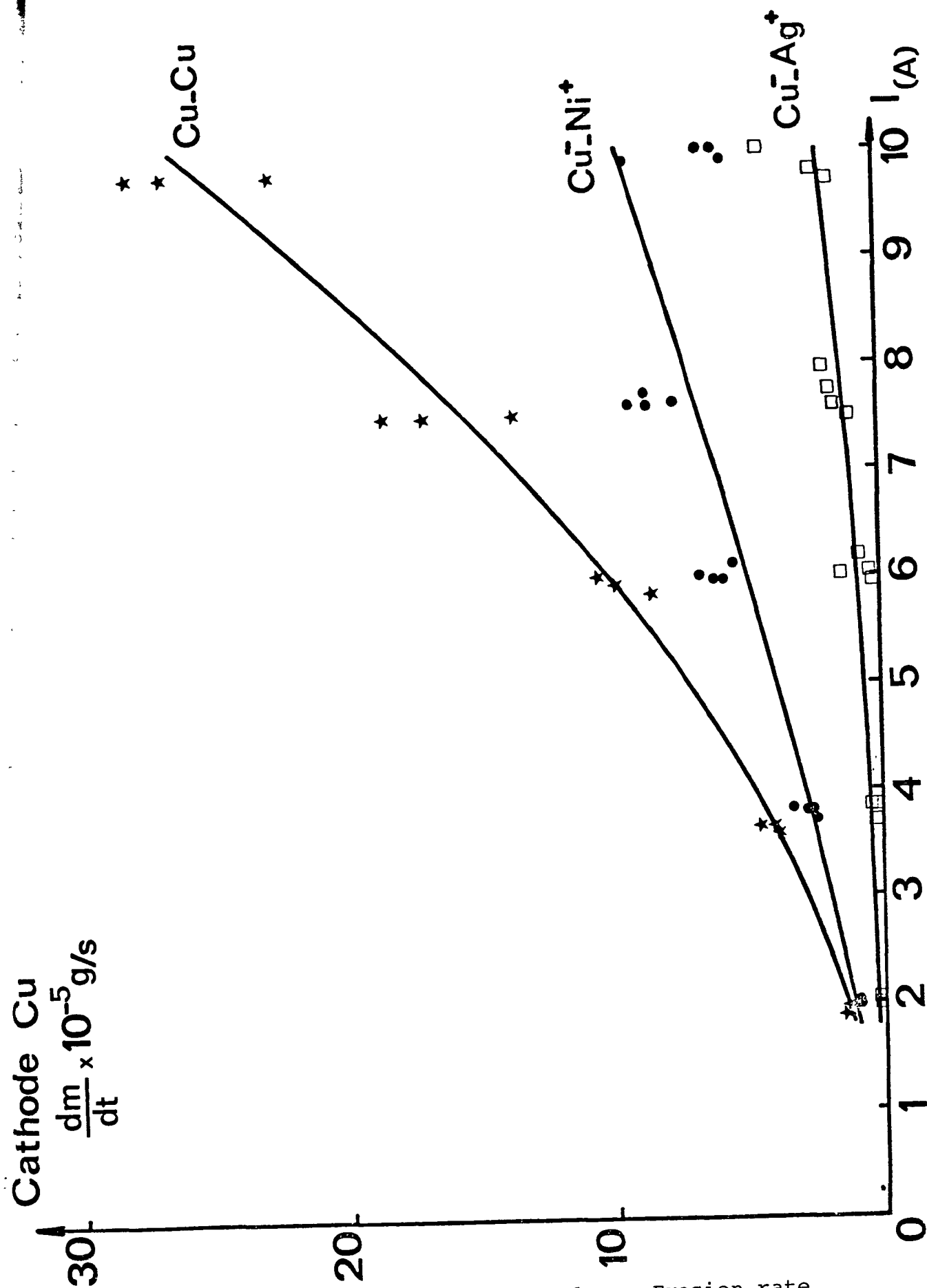Figure 19 - Dissymmetrical couples. Erosion rate of a nickel cathode

55

44

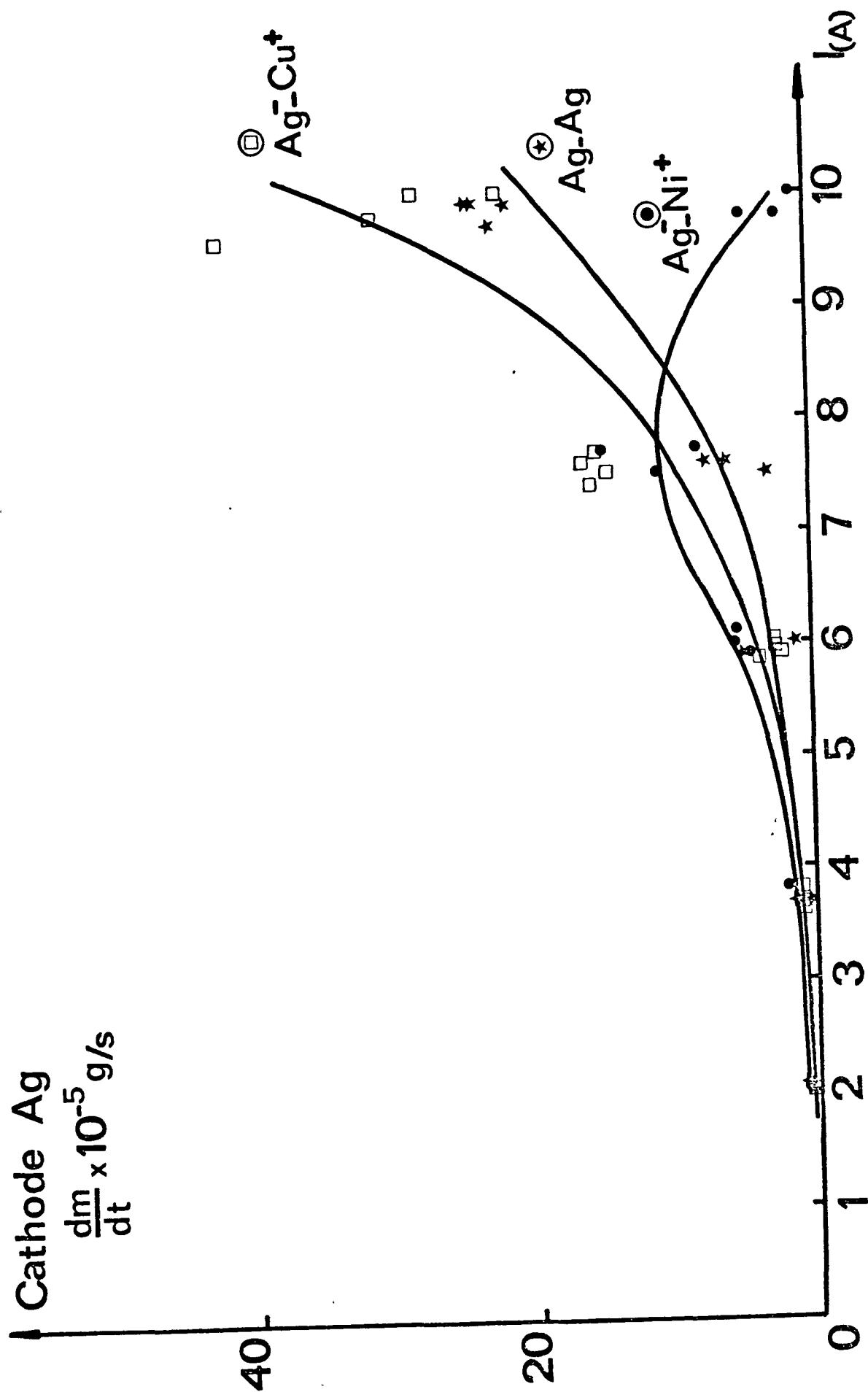Figure 20 - Dissymmetrical couples. Erosion rate
of a copper cathode.

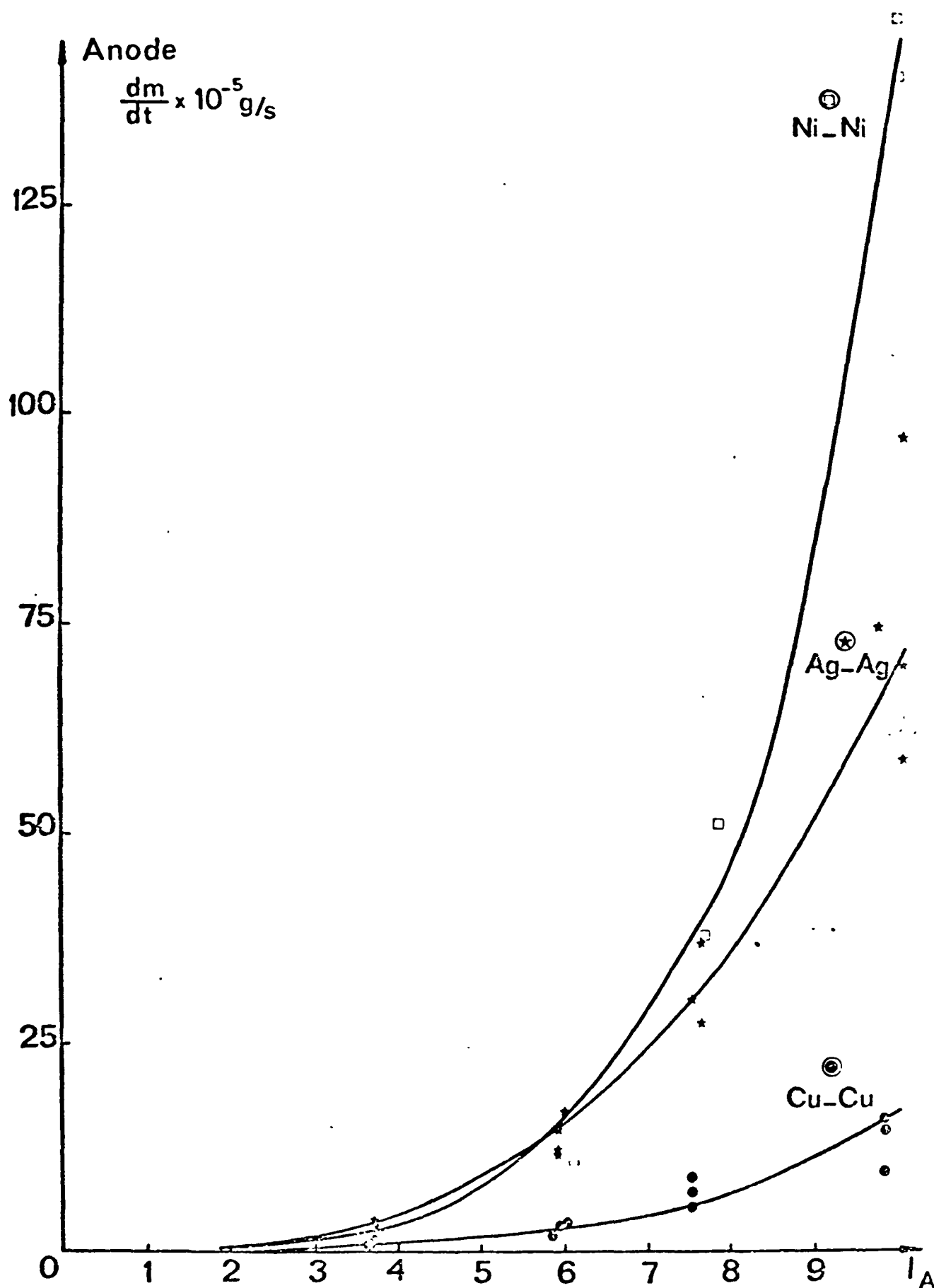Figure 21 - Dissymmetrical couples. Erosion rate of a silver cathode.

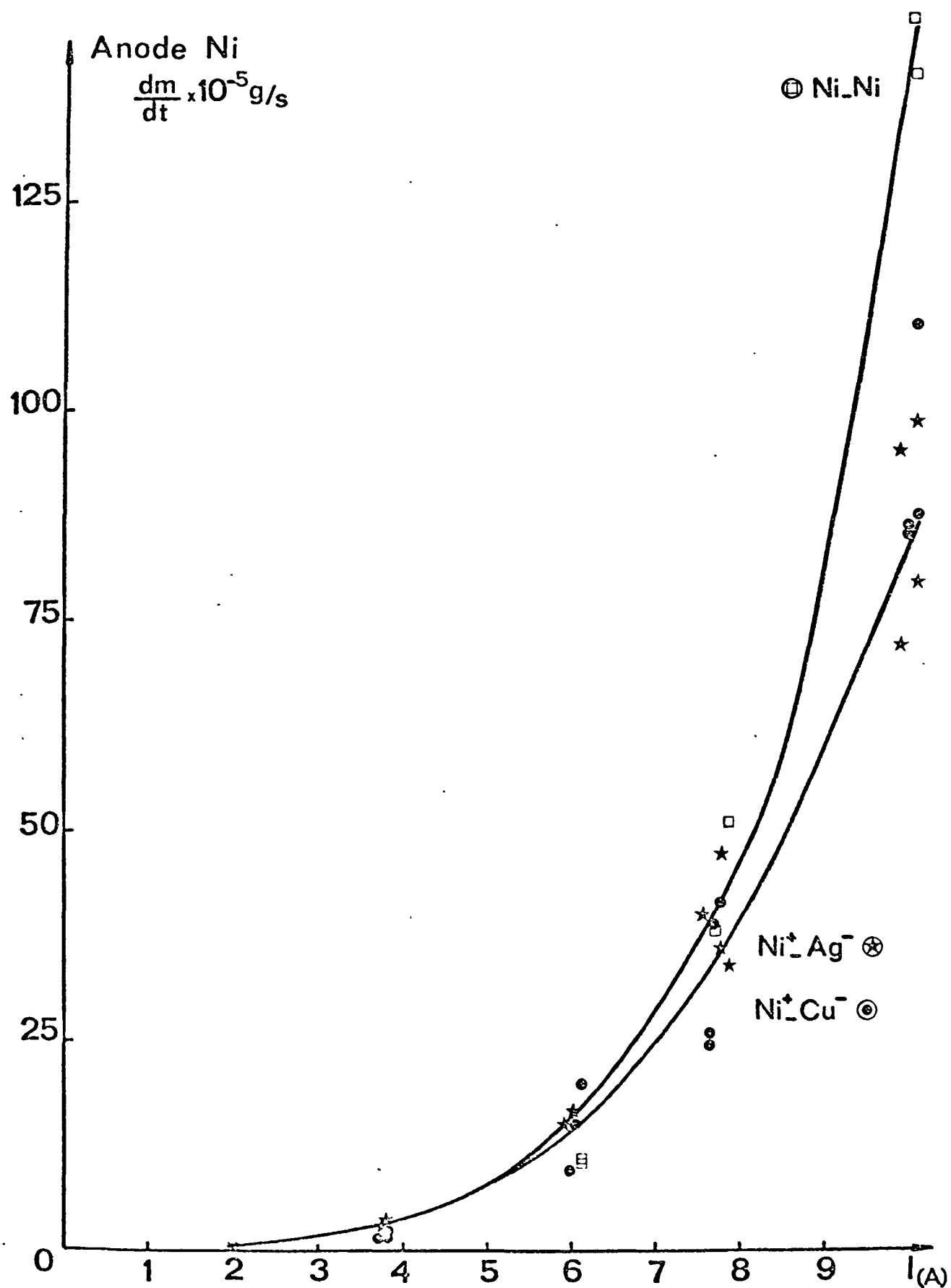Figure 22 - Symmetrical Couples. Anode erosion rate.

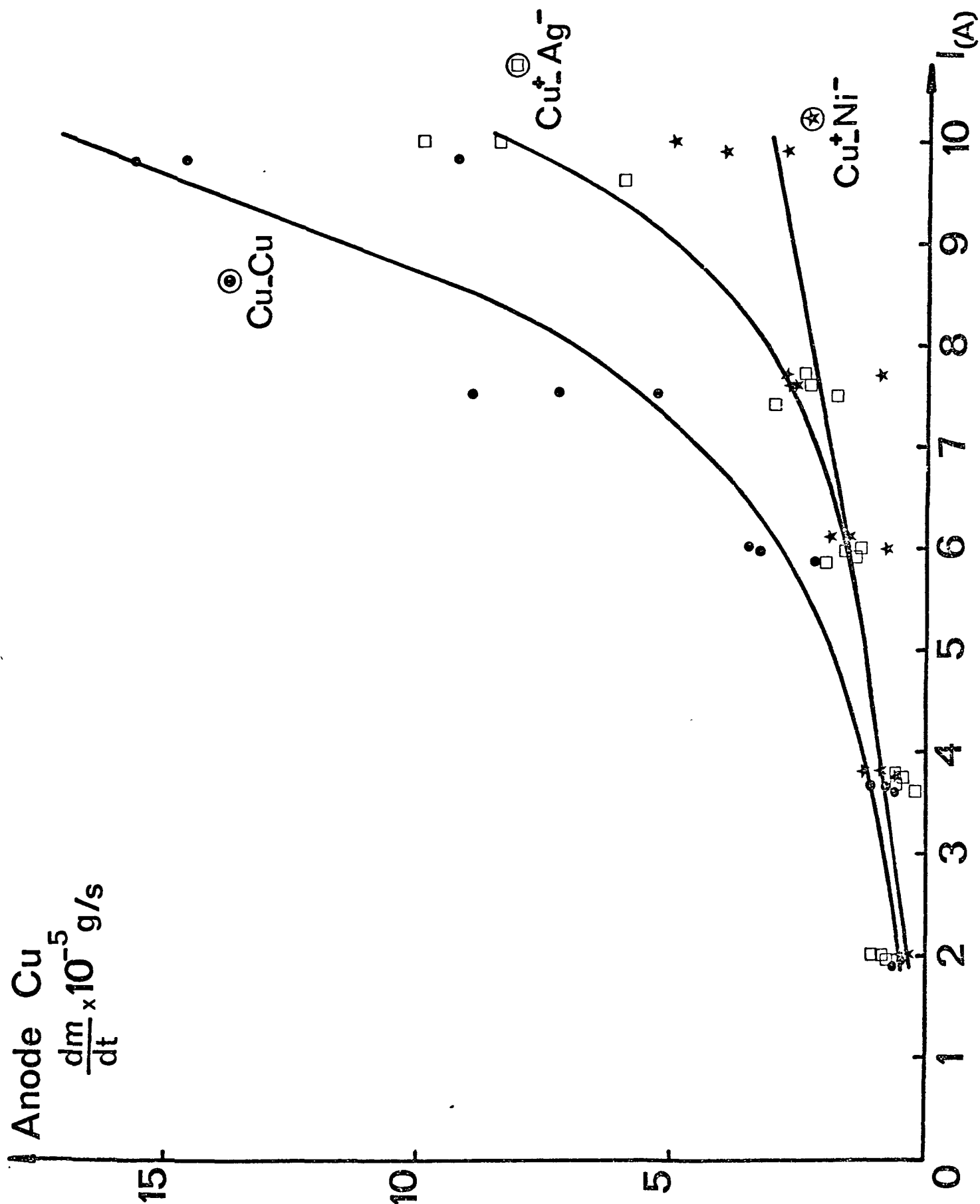Figure 23: Dissymetrical couples. Erosion rate of a nickel anode.

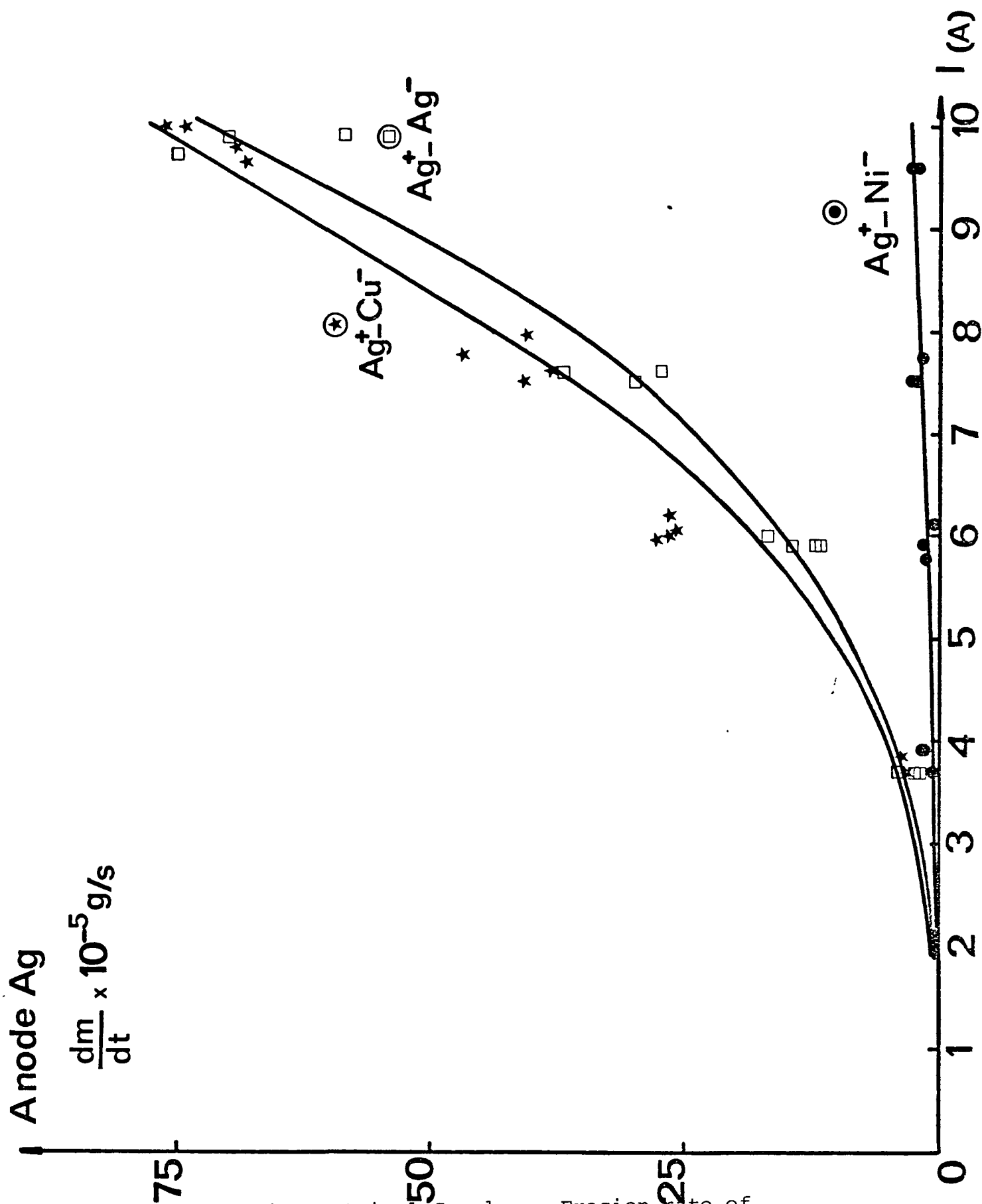Figure 24 - Dissymmetrical Couples.   Erosion rate of
a copper anode.

Figure 25 - Dissymetrical Couples. Erosion rate of
a silver anode.

b)   Dissymmetrical Couples

Nickel cathodes exhibit virtually the same erosion rate for the /63
three types of anodes. The anode would therefore have no influence
on the wear of the nickel cathode.

Copper cathodes show erosion rates which vary with the type of
anode. There is less erosion when the anode is of a different nature
than that of the cathode.

Silver cathodes have erosion rates which vary with the type of
anode used. The erosion rate has a maximum level of I = 7.5A and
decreases with strong currents in the case of a silver-nickel couple.

This shows the affect of the anode type on the cathode wear.

5.4.2.2 - Anodes

a)   Symmetrical Couples

Little work has been devoted to anode wear and its role in the
arc's behavior, based on the assumption that the anode would play a
passive role.

In the case of the Nickel-Nickel, couple, the rapid decrease in
anode wear is mainly due to the metal conversion into an oxide, which
is a loss. In the case of the Silver-Silver couple, the anode eros-
ion is greater than that of the cathode. Furthermore, the experimen-
tal points are much more scattered. Visual observation of the elec-
trode shows us that one part melted and that the metal could be rand-
omly ejected in liquid form. This causes the high current points to
scatter.

With the Copper-Copper couple, there is less erosion on the   /64
anode than on the cathode.

b) Dissymmetical Couples

The nickel anodes have a lower erosion rate when the cathode is made of silver or copper than when the cathode is made of nickel.

The same is true for copper, i.e. there is less erosion on the copper anode with silver or nickel cathodes than with a copper cathode.

With silver andoes, one finds virtually the same erosion rates with copper cathodes as with silver cathodes. Conversely, with a nickel cathode, everything happens as if the nickel eroded leaving silver intact, as in the case of the copper anode nickel cathode, leading to an unusually low silver erosion.

5.4.3 - SUMMARY DIAGRAM

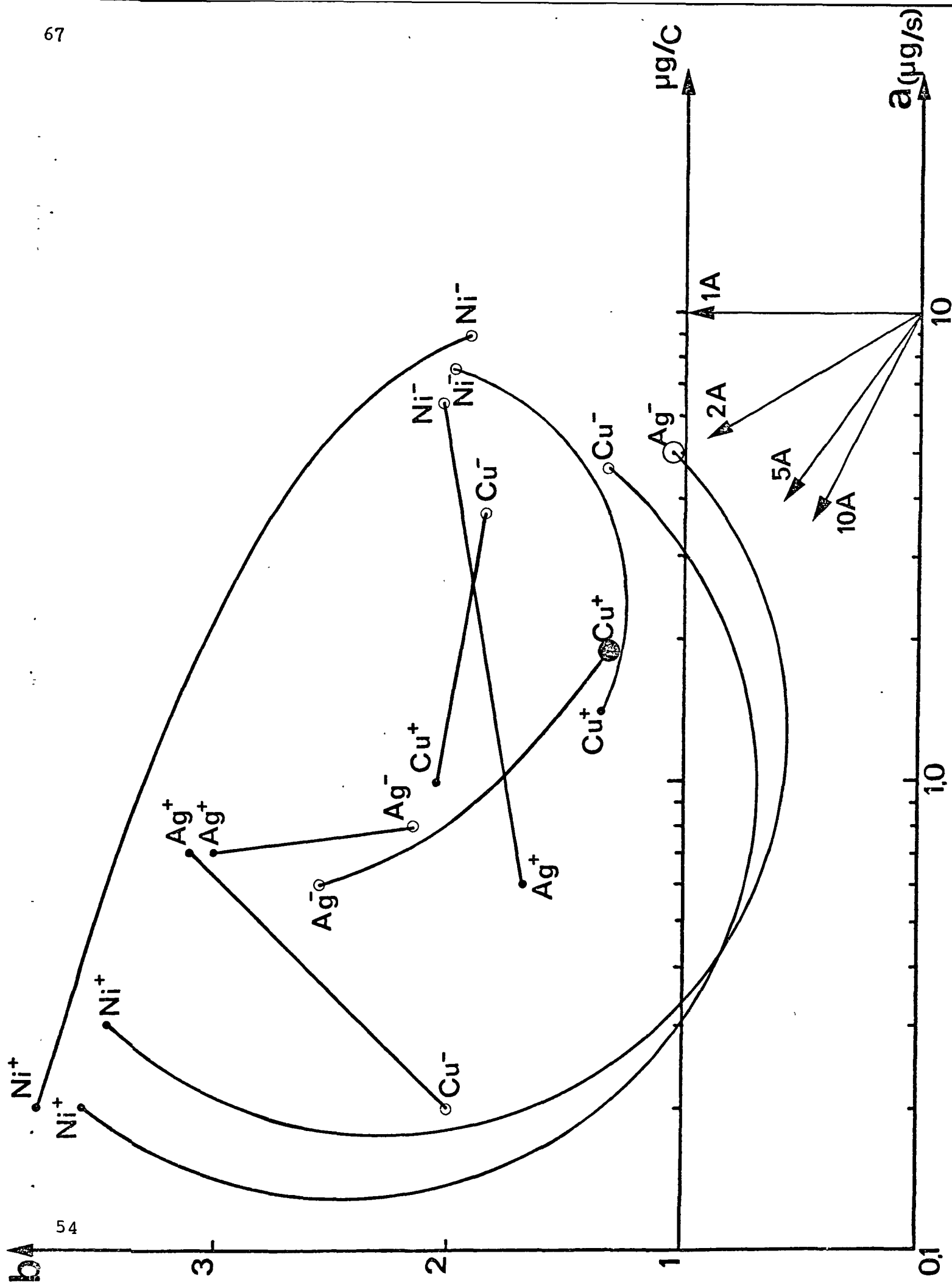Given the curve appearance, we decied to use the following empirical law to represent them:

$$\frac{dm}{dt} = al^b \tag{1}$$

The adjustment of a power function to a set of points $|\frac{dm}{dt}|_i$, I_i using the least squares method gives us coefficients a and b. On the following table we showed the values obtained for a and b as well as the regression coefficient R^2. The adjustment is generally good, except for the Cu^+ and Ar^- electrodes where the regression coefficients are low.

To represent all results of the table, we use a semilogarithmic graph where the x-axis is the logarithm of a and the y-axis of the b value. Each curve corresponding to each electrode of a couple is represented by a point. The two points of a couple are connected by a line to relate them.

The graph adopted is used to work out the erosion rate using

ANODE	ANODE		
CATHODE	Ag	Cu	Ni
Ag	a = 0,07 b = 3,01 R^2 = 0,98	a = 0,19 b = 1,31 R^2 = 0,58	a = 0,03 b = 3,46 R^2 = 1,00
	a = 0,08 b = 2,15 R^2 = 0,72	a = 0,06 b = 2,55 R^2 = 0,88	a = 0,50 b = 1,05 R^2 = 0,42
Cu	a = 0,07 b = 3,11 R^2 = 0,99	a = 0,10 b = 2,05 R^2 = 0,90	a = 0,02 b = 3,56 R^2 = 0,98
	a = 0,02 b = 2,01 R^2 = 0,81	a = 0,37 b = 1,85 R^2 = 0,99	a = 0,46 b = 1,32 R^2 = 0,90
Ni	a = 0,06 b = 1,68 R^2 = 0,92	a = 0,14 b = 1,35 R^2 = 0,85	a = 0,02 b = 3,74 R^2 = 0,97
	a = 0,64 b = 2,03 R^2 = 0,97	a = 0,74 b = 1,99 R^2 = 0,99	a = 0,89 b = 1,92 R^2 = 0,90

a simple graph construction. In effect, from the relationship

$$\log\left(\frac{dm}{dt}\right) = \log(a) + (\log I)\, b \tag{2}$$

we see that $\log\left(\frac{dm}{dt}\right)$ is a linear function of $\log(a)$ and b. By grad-
uating the x-axis with g/s we may obtain the erosion rate by plot-
ting a straight line based on the representative point and with a
slope wall to $\log(I)$.

We all see that like:

$$\frac{dm}{dq} = \frac{dm}{dt}\ \frac{dt}{dq} = \frac{1}{1}\ \frac{dm}{dt} \tag{3}$$

the erosion expressed in g/C is derived from relationship (1) via

$$\frac{dm}{dq} = aI^{(b-1)} \tag{4}$$

This equation is shown on the chart using the same points, in a new
system of axes where the y-axis is decreased by one, while the graph
construction remains the same.   The regression coefficients were
kept by representing them with a larger circle.

Nickel, whether it be a cathode or anode, erodes independently
of the type of metal used on the other electrode.

The Ag^+'s depend very little on the type of metal used on the
cathode if it is in copper or silver, but this wear is much less
sensitive to the current increase wehn the cathode is in nickel.
Likewise, Cu^+ depends very little on the cathode type if it is in
Ag or Ni.

The points are very scattered for Cu^-, and there is very little
erosion when the anode is in Ag.

The Ag^-'s are very scattered and the erosion rate is very low

in the case of the Ag^- - Ni^+ couple.

The results appear in the form of $\frac{\Delta m}{\Delta \emptyset}$ curves where Δm is the amount of matter lost in time Δt and $\Delta \emptyset$ is equal to $\overline{I}_{ij} \Delta t$ from relationship (23) in chapter 3.

5.5.1 - Cathode

For nickel, there is a correlation between the mass lost by the cathode and the line intensity for the current range under study.

This ratio exists for silver as of 5A. Below this value, the curve takes on larger values, which could mean that part of the material would leave in the form of aggregates without being excited. The same thing is found for copper, but this time the ratio starts as of 6A.

5.5.2 - Anode

This proportionality does not exist for the anode as it does for the cathode, as the values are highly scattered. This is because the oxides formed on the anode do not enrich the steam arc and increase the spectral line intensity, but form a metal loss. This process may lead to an increase in the electrode mass. To eliminate this cause of error the electrodes are cleaned, before being weighed, after being subjected to the arc effects.

The process by which the anode injects steam into the arc is indirect since it occurs in 2 phases: conversion of the metal into   /73 an oxide, then vaporization and decomposition of the oxide.

The oxidation process is inadequately controlled in arc devices, because it depends on the anode temperature, the type of surrounding gas, the metal's reactivity and, as we have seen, the
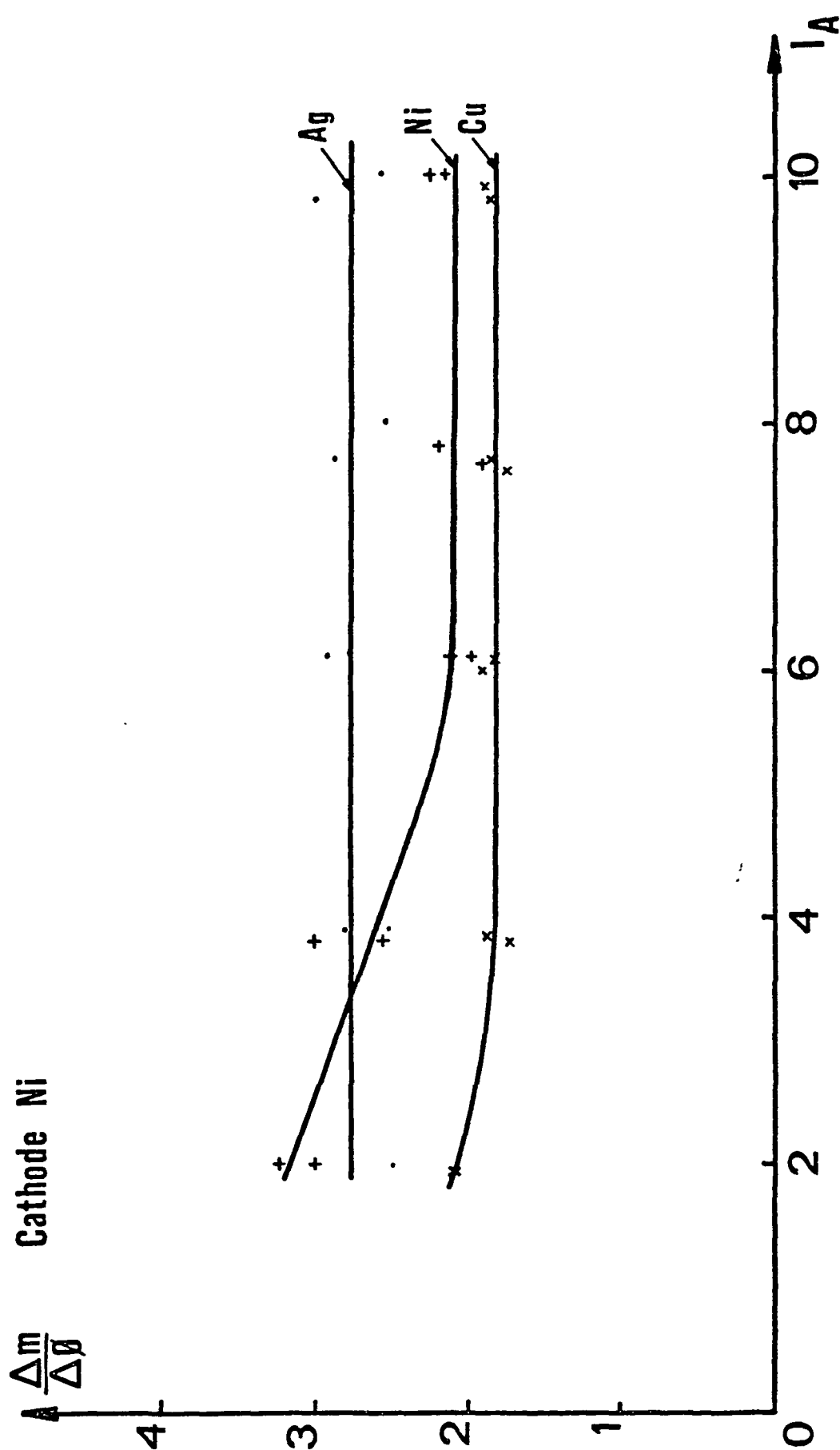
Figure 26 - Variation in the ratio between the erosion rate and the intensity of a spectral line as a function of the current. Case of a nickel cathode.
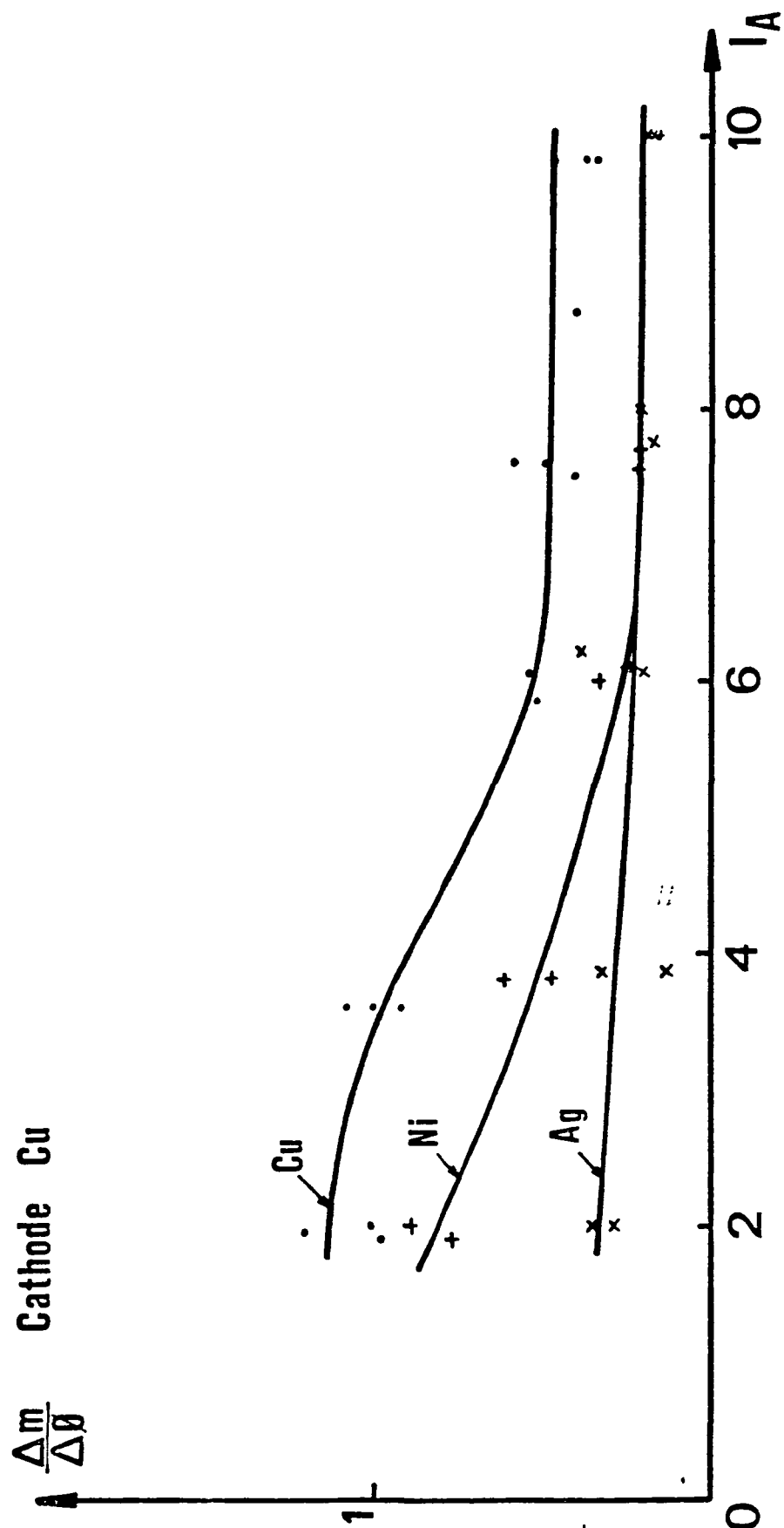
57

Figure 27 - Variation of the ratio between the erosion rate and intensity of a spectral line as a function of the current. Case of a copper cathode
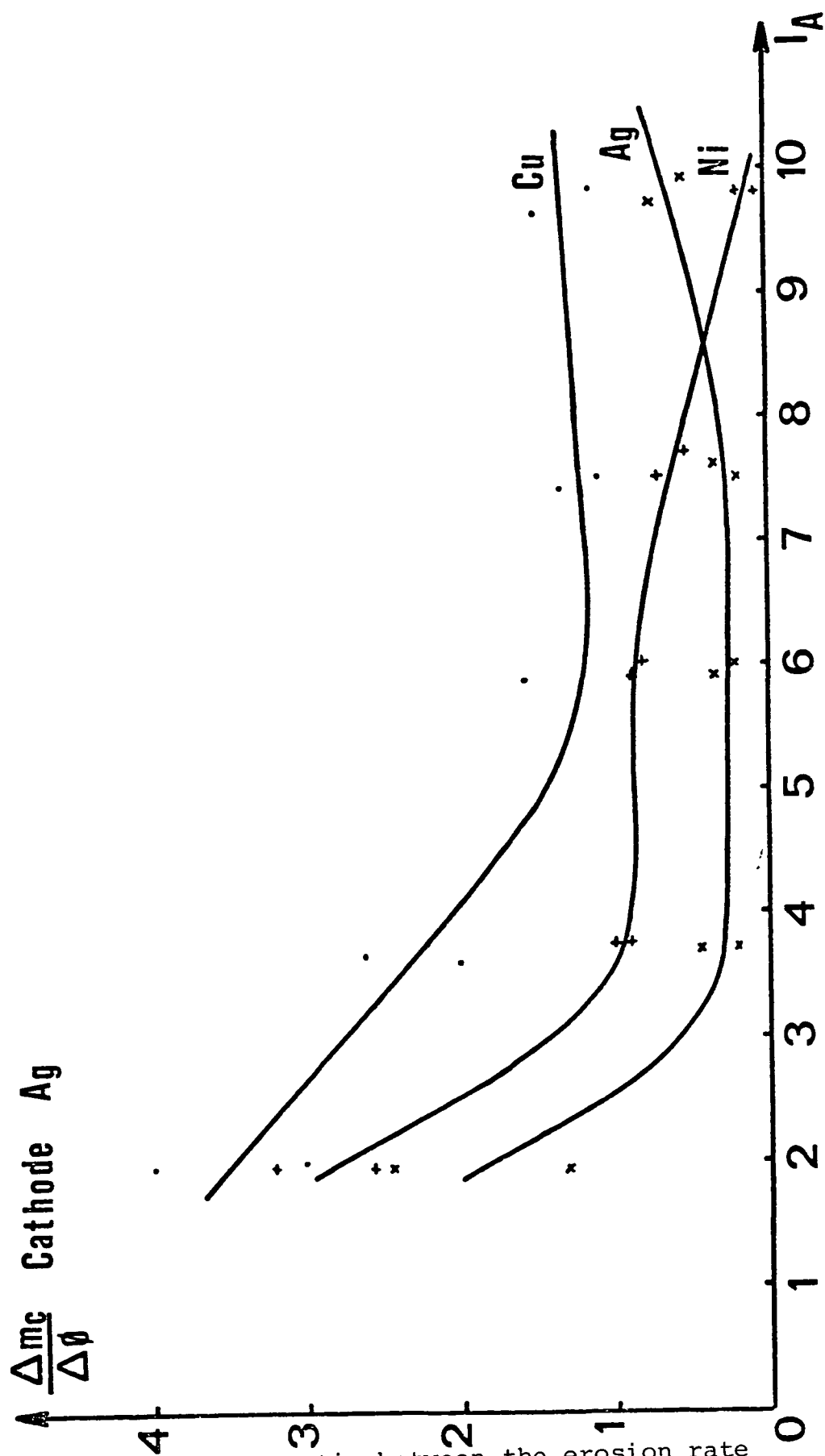
Figure 28 – Variation of the ratio between the erosion rate and the intensity of a spectral line as a function of the current. Case of a silver cathode.

type of metal used on the cathode.

CHAPTER 6 - CONCLUSION

We developed and used a method for measuring the erosion rate of electrodes in a arc due to the intensity of a spectral line emitted. It was demonstrated that 2 factors must be taken into account which may influence it. The first factor is the plasma temperature. We determined its law of variation due to the relative intensity ratio and showed that this ratio is constant in the current range used.

The other factor is the optical transparency of the medium at the wavelength of the line selected. To measure it, we altered the conventional method of using a concave mirror which allowed us to cross the arc's movement.

We tested this method of measuring the erosion rate with three metals. Due to the various roles played by the cathode and the anode, we tested 9 different electrode combinations. Despite a great discrepancy in the results, the method may be used for determining cathode erosion. Further, it was shown that the type of metal used on the anode influences the cathode erosion.

These studies allowed us to show that certain dissymetrical couples exhibit a very low erosion of noble metals (Ag) which seems advantageous for applications of this technique to contactors.

On the assumption that the erosion rate is propoptionatl to
the current, we built a chart which allowed us to select a pair of electrodes.

REFERENCES

1   BADEREU-POPESCU: "Ionized Gas", Dunod, Paris 1968.

2   J. Lowke, Proceedings of the XIIth ICPIG, Eindhoven 1975.

3   A.von Engle, "Ionized GAses", 2nd edition, Oxford 1965.

4   KESAEV I., Sov.Phys.Tech.Phys. Vol. 9, no. 8, 1146, 1965.

5   R. Fowler, L. Nordheim, Proc.Roy.Soc. A 119, 173 (1928).

6   S. Mackeown, Phys.Rev. Vol, 34, 611, 1929.

7   E. Murphy and Jr Good, Phys.Rev. 102, No. 6, 1964 (1956).

8   Th Lee, Th. Lee, J.Appl.Phys. 30, 166, 1959.

9   F. Rohrback, Thesis, Lausanne 1971.

10 G. Ecker, Ergebn.Exakt.Naturw. 1961, 33 pp 1-104.

11 H. Hagstrum, Phys.Rev. 96, 325, 1954; 104-317, 1956.

12 Weissler, Handbuch der Physik (Springer 1956) Vol. 21, p 376

13 Von Engle and Robson, Proc.Roy.Soc., 1957 (A), 242, p 217

14 A. Holmes, J.Phys.D.Appl.Phys., Vol. 7, 1974.

15 Bez W. and Hocker K. Z. Naturforsch, 99, 72 (1954).

16 C. Kimblin, J. of Appl. Phys., Vol. 45, No. 17, 5235 - 5244, 1974.

17 C. Kimblin, J. of Appl. Phys. Vol. 44, No. 7, 3079 - 3081, 1973.

18 Guile A. and Hitchcock A., J. Phys. D, Vol, 8, 1975 pp 663-669.

19 Dikson D. and von Englen A. Proc.Roy. Soc. 1967 (A) 300, p 316-325.

20 V. Grakov, Sov. Phys. Tech. Phys. Vol. 12, No. 2, 286, 1967.

21 Szabo I., Apectrochimica Acta, Vol, 2-B, p 231-239, 1974.

22 Rich J. J. Appl, Phys, Vol. 32, No. 6, 1023, 1961.

23 Guile A., A. Hitchcock A, Proc. IEE, Vol, 122, No. 9, 950, 1975.

24 Lee Th, J. Appl. Phys, Vol, 31, No. 5, 924, 1960.   /77

25 Cobine, B. J.Appl.Phys, 26, 895, (1955).

26 Gray E. Pharney J., J. Appl. Phys. Vol. 45, No. 2, 1974, p. 667-671.

27 Drouet M. Gruber J., IEEE Trans. P.A.S. 95, 105 (1976).

28 Mitterauer, Proc. 11th ICPIG, Prague, 1971, p. 70.

29 Drawin H. Felenbok P. "Data for Plasmas in L.T.E. (Gauthiers-
    Villars), Paris 1965.

30 Vujnovic V. J.Q.R.J.T., Vol, 13, p. 14651477 (1973).

31 Marton L, "Methods of Experimental Physics", vol. 7, Part. B,
    Chap. 7, Academic Press, 1968.

32 Griem H. Phys. Rev. 131, 1170 (1963).

33 Miyachi J. and Assoc., J.I.E.E. of Japan, June 1967, p. 1227.

34 Turner H. and Turner C. ERA Report 1966.

35 Guile A. and Hitchcock, J. Phys. D: Appl. Phys., Vol. 8, p. 427, 1971.

36 Buchet G., in print.

37 Gilmore J.Q.S.R.T, Vol, 5, p. 125, 1965.

38 Zel'dovich Ya. and Raizer Yu, "Physics of Shock Waves and High Temperatures. Hydrodynamic Phenomena, Vol, I, Academic Press 1966.

39 Shayler P. and Fang M., ULAP Report - T45 December 1976.

40 Cobine J. and Gallagher C., "Phys. Rev. Vol, 74, No. 10, November 15, 1948, p. 1524.